JOURNAL OF MATERIALS SCIENCE **40** (2005) 819–839

Cornerstones of grain structure evolution and stability: Vacancies, boundaries, triple junctions

L. S. SHVINDLERMAN
Institut für Metallkunde und Metallphysik, RWTH Aachen, D-52056 Aachen, Germany; Institute of Solid State Physics, Russian Academy of Science, Chernogolovka, Moscow, distr., 142432 Russia

G. GOTTSTEIN*
Institut für Metallkunde und Metallphysik, RWTH Aachen, D-52056 Aachen, Germany
E-mail: gottstein@imm.rwth-aachen.de; http://www.imm.rwth-aachen.de

The paper is dedicated to a major topic of Grain Boundary Engineering: evolution and stability of granular microstructures. The various mechanisms of grain microstructure stabilisation are considered. The role of grain boundaries, vacancies and especially triple junctions as dragging factors in grain growth of polycrystals is comprehensively discussed. A hierarchy of efficiency of different mechanisms for grain growth inhibitionis presented. It can be utilized as a basis for an assessment of the stability of fine grained and nanocrystalline materials.

1. Introduction

A paper published in this special issue dedicated to Grain Boundary Engineering (GBE) should reflect this direction or develop it. GBE declares a possibility of control or, at least, of directed change of the properties of a material through the formation of an optimal distribution of grain boundaries with special properties. This concept has been embodied in the papers of the groups of Watanabe, and Palumbo, respectively [1–5]. The practical realization of this idea was reduced to thermomechanical treatment, most often to the thermocycling. Such treatment results in an increase of the number of special grain boundaries, predominantly twin boundaries. While not questioning the prospects of such approach the authors would like to call the reader's attention to the fact that a deeper understanding of well known processes or physical phenomena which permit us to create materials with given properties and (or) distribution of grain boundaries is subsumed under GBE as well. Strictly speaking, all processes which transform the properties of materials due to a change in grain boundary properties and distribution, in other words, in grain microstructure—recovery, recrystallization and especially grain growth—fall in this category. This is our understanding of GBE. We will, in particular, consider the latter, namely grain growth. Grain growth defines the change of grain microstructure as a function of internal parameters of the sample—chemical nature of the matrix, material impurities, composition—and the characteristics of the process—temperature, pressure, duration of annealing. Finally, to generate the desired grain microstructure is only half of the problem. The next step is to retain, i.e. to stabilize the formed microstructure. This issue is of especial importance for fine grained and nanocrystalline materials.

2. "Equilibrium" grain size in the system with impurity

It is common knowledge that grain boundaries are non-equilibrium defects in crystalline solids. In other words, there is no equilibrium grain size for a polycrystal. Actually, the free energy for a pure polycrystal can be expressed as:

$$\Delta G = \Delta G(T) + \gamma(T)\mathbb{S} \tag{1}$$

The first term on the right-hand side of (1) defines the energy of the bulk of the polycrystal while the second term constitutes the grain boundary energy, i.e., the product of grain boundary area $\mathbb{S}$ and grain boundary surface tension γ. If $\gamma > 0$ there is no special grain size for which relation (1) has a minimum (extremum). This brings up the question: Is there an equilibrium grain size in a system with impurities, in particular in a binary system?

$$\Delta G = \Delta G_{\text{sol.}}(T, c_2) + \gamma(T, c_2)\mathbb{S} \tag{2}$$

Kirchheim [6] provided a positive answer to this question. His consideration is based on classical J. W. Gibbs approach where the properties of the bulk of the system, the "reservoir", are constant in the course of displacement of atoms from the interface to the bulk and back. Briefly the arguments of R. Kircheim can be expounded in the following way. Transfering a small amount of

*Author to whom all correspondence should be addressed.

impurity from the bulk solid solution to the interface increase the free energy of the bulk solution and at the same time decreases the free energy of the interface. In other words the free energy of a system with an interface might have an extremum. (It is desirable to have a minimum). On the other hand the free energy of a system without interface is obviously smaller than with the interface. The question is whether the surface tension of an interface can vanish during the impurity adsorption. Kirchheim [6] reasones that such process is possible.

3. Kinetic "Stabilization" of grain microstructure

A thermodynamically stable grain size is unlikely even in a system with impurities. Michels *et al*. [7] discussed the feasibility to apply the Burke model [8] to the grain growth in nanocrystals. The peculiarity of grain growth in fine grained and nanocrystalline materials is that the increase of the mean grain size and correspondingly, the reduction of the total grain boundary area results in a tangible redistribution of the impurities—the bulk concentration increases, and by doing so raising boundary adsorption. The Burke model is based on the assumption that the drag force is determined by a maximal grain size $\bar{R}_{\max}$. Grain growth ceases as $\bar{R}_{\max}$ is approached. Michels *et al.* [7] found that for fine grained materials the difference of the impurity concentration at the boundary and in the bulk changes linearly with respect to the mean grain size. Then the maximum radius $\bar{R}_{\max}$can be extracted from the relation:

$$\frac{d\bar{R}}{dt} = m_{\mathrm{b}}\left(\frac{\alpha\gamma}{\bar{R}} - f\right) \tag{3}$$

where f is a drag force which is proportional to mean grain size which, in turn, scales with the mentioned difference of concentration in the bulk and at the grain boundary: $f = \chi\bar{R}$, where χ is a constant. Hence the limiting radius $\bar{R}_{\max} = (\frac{\alpha}{\chi}\gamma)^{1/2}$. Rabkin [9] called attention to the fact that the authors of [7] did not take into consideration the dependence of the drag force on grain boundary velocity (grain growth). The latter dependence was accounted for in all theories of impurity drag on grain boundary motion [10]. In this case

$$f = \chi'\bar{R}\frac{d\bar{R}}{dt} \tag{4}$$

with χ' a new constant. Accordingly, there is no more a limiting grain size $\bar{R}_{\max}$.

This conclusion is doubtful, however, since the authors of [7] used the Burke model in which the existence of the limiting grain size was assumed from the outset [8]. Burke believed that the reasons for dragging of boundary motion are impurities, surface of the sample, and second phase particles. In other words, the case in point is the strong dragging of grain growth other than complete termination of the process. Secondly, Equation 4 is valid for $\bar{R} \sim \Delta C = C_{\mathrm{b}} - C_2$, where C_{b} is the impurity concentration at grain boundary, C_2 in the bulk, respectively. However, obviously this relation is valid for sufficiently small grain size only.

$$C_2 = \frac{V_0 c_2^0 - \Gamma_2 S}{V_0} \tag{5}$$

where V_0 is the volume of a sample, Γ_2 is the value of the impurity adsorption at grain boundaries, c_2^0 is the average impurity concentration in the sample. Just this concentration should be used when the bulk free energy of a solid solution is evaluated.

Since at least for not so large concentrations $C_{\mathrm{b}} = BC_2$, B is an adsorption coefficient

$$\begin{aligned} C_{\mathrm{b}} - C_2 &= (B-1)\frac{V_0 C_2^0}{V_0 + \frac{3}{2}\cdot\frac{\delta}{\bar{R}}(B-1)} \\ &= \frac{2R(B-1)V_2 C_2^0}{2\bar{R}V_0 + 3\delta(B-1)} \end{aligned} \tag{6}$$

Only for sufficiently small $\bar{R}$, as mentioned in [7], $C_{\mathrm{b}} - C_2 \sim \bar{R}$. In other words, both Equation 8 with $\bar{R}_{\max}$, used in [7], and Equation 9 [4] refer to a sufficiently small grain size.

We think, it is of interest to consider also a situation when the excess of impurity which is acquired due to grain growth causes the formation of second phase particles, first of all at the grain boundaries. In this case at some critical $\bar{R}$ the concentration of impurities in the sample exceeds the solubility limit, precipitation of the second phase particles will start and grain growth will be slowed down.

Rabkin [9] considered a situation where grain boundaries are saturated with impurities from the outset. In accordance with [9] the particles contain impurity atoms only. These particles are randomly distributed along the GB network and exert pinning force on the moving GB. Small particles are dragged along by migrating grain boundaries by mechanisms of interfacial diffusion while sufficiently large particles move together with grain boundaries by the mechanism of bulk diffusion, or they detach from the grain boundary [10, 11]. If all particles nucleate at the beginning of grain growth, as assumed in [9] and the accommodation of impurities occurs exclusively by the growth of existing particles, then the equation of joint motion of grain boundary and particles reads:

$$\frac{d\bar{R}}{dt} = m_{\mathrm{b}}\left(\alpha\frac{\gamma}{\bar{R}} - f(r)n_0\frac{\bar{R}}{\bar{R}_0}\right) \tag{7}$$

where $f(r) = \pi r\gamma\sin(2\varphi)$ is the interaction force between grain boundary and a particle, φ is the angle between the tangent to the grain boundary at the point contact and the normal to the direction of grain boundary motion, n_0 is the number of particles per unit area, $\bar{R}_0$ is the initial grain size, r is the radius of the particle. In [9] the joint motion of grain boundary and particles was described by the equation:

$$\frac{d\bar{R}}{dt} = m_{\mathrm{p}}(r)f(r) \tag{8}$$

$m_p(r)$ is the particle mobility. With Shewmon's expression for $m_p(r)$ [10]:

$$m_p(r) = \frac{\Omega_a D_S \delta}{kTr^4} \tag{9}$$

Ω_a, D_S, δ are the atomic volume, the interfacial diffusion coefficient and the thickness of the interfacial layer in which the diffusion occurs, respectively.

The system of Equations 7–9 together with the expression for the conservation of the impurity atoms determines the behavior of the system considered. The main result can be expressed as:

$$\sin(2\varphi) = \frac{A}{\varsigma} \cdot \frac{1 - \frac{1}{\varsigma}}{1 + B\varsigma\left(1 - \frac{1}{\varsigma}\right)^{4/3}} \tag{10}$$

where $\varsigma = \frac{\bar{R}}{\bar{R}_0}$, $A = \frac{9kTc_0 m_b}{8n_0\pi^2\Omega_a D_S \bar{R}_0}$, $B = \frac{kTn_0 m_b}{\Omega_a D_S}\left(\frac{3c_0}{4\pi n_0}\right)^{4/3} \cdot \delta$, c_0 is the impurity concentration in the saturated grain boundary layer. It is the authors' opinion that the value of $\sin(2\varphi)$ is an indicator of the regime of grain boundary motion. Namely, when $\sin(2\varphi) < 1$ the grain boundary moves together with the particles. In the range of $\sin(2\varphi) > 1$, the grain boundary detaches from the impurities. It is important to note that A in Equation 10 is inversely proportional to the initial grain size $\bar{R}_0$. This means that after each detachment grain growth will be described by the same set of equations but with a smaller value of the parameter A. Rabkin [9] states that neither impurity drag nor particle drag can stop completely grain growth in a polycrystal, however they are able to essentially slow down this process. Going along with this statement we would, nevertheless, like to stress that in [9] not the joint motion of grain boundary and particles was considered but a dissociation of grain boundary and particles. Actually, a comprehensive theory of joint motion of grain boundary and particles [11] showed that Equation 8 defines the maximum interaction force between grain boundary and particles, associated with the last moment of joint motion.

4. Grain growth accelerated by precipitation

In this context we raise the question whether the formation of a second phase always slows down grain growth in polycrystals, in particular in nanocrystals. Let us consider an effect associated with grain boundary motion, or, more correctly with grain growth in a solid solution [12]. When the sample (polycrystal) is in a single phase field grain boundary motion, or the rate of grain growth, is described by the theories of impurity drag—Lücke-Detert, Cahn, Lücke-Stüwe [10]. However, if we lower the temperature by ΔT or change the concentration by Δc (Fig. 1) the system enters the two-phase field. In spite of the apparent degradation of the conditions for grain growth, the migration rate may be higher if the drag effect of the second phase particles will be smaller than the reduction of impurity drag, owing to the depletion of the solid solution. Experimentally this effect manifests itself in an apparent negative activation energy or in an increase of the grain growth rate with rising concentration. Obviously, this effect is only feasible when special conditions are met. By decreasing the temperature by ΔT we offset the system to the two-phase field and the fraction W_p of the particles with respect to the solid solution $W_{sol.sol.}$ will be equal to (Fig. 1):

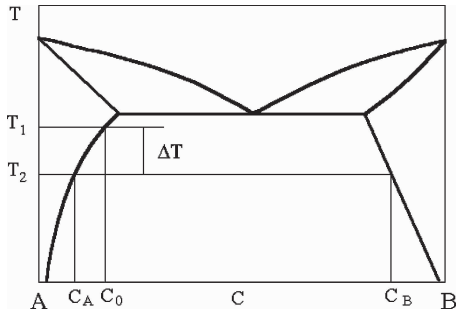

Figure 1 Eutectoid binary phase diagram.

$$\frac{W_p}{W_{sol.sol.}} = \frac{c_0 - c_A}{c_B - c_0} \tag{11}$$

In the two-phase field the equilibrium concentration of the solid solution will be $c_0' = c_A$ (Fig. 1).

The requirement of accelerated growth demands

$$V(c_0' = c_A, particles) > V(c_0) \tag{12}$$

Two situations will be considered. The first one relates to a system with large, immobile particles. In this case the grain growth rate can be represented as:

$$V = m_b[P - P_{im}(V) - P_p] > m_b[P - P_{im}(V)] \tag{13}$$

where† $P = \frac{\alpha\gamma}{\bar{R}}$ is the driving force for grain growth, P_{im} and P_p are drag forces due to solute atoms and by immobile particles, respectively. To assess relation (17) we will use the Zener [10] and Lücke-Detert [10] approximations:

$$P_p = \frac{3f\gamma}{r} \tag{14}$$

$$P_{im} = \Gamma\frac{V}{D_{im}}kT \tag{15}$$

where f is the volume fraction of the particles, Γ—the adsorption at grain boundaries, D_{im}—bulk diffusion coefficient of the impurity. For grain growth in a solid solution we arrive at:

$$V = \frac{m_b P}{1 + \Gamma(c_0)\frac{kT}{D_{im}}m_b} \approx \frac{D_{im}P}{kT\Gamma(c_0)} \tag{16}$$

† Usually the radius of grain curvature during grain growth does not agree with the mean grain size $\bar{R}$ as accounted for the coefficient α, which is different from 3/2. However, for sake of simplicity we assume that $\alpha = \frac{3}{2}$.

and for grain growth in a solid solution with second-phase particles we obtain:

$$V = \frac{m_b\left[P - \frac{3f\gamma}{r}\right]\frac{D_{im}}{kT}}{\Gamma(c_0' = c_A)} \tag{17}$$

An acceleration of grain growth caused by the formation of second-phase particles will fit the relation:

$$\frac{P - \frac{3f\gamma}{r}}{\Gamma(c_0' = c_a)} > \frac{P}{\Gamma(c_0)} \tag{18}$$

The relation (22) is valid under the assumption that the impurity diffusion coefficient is independent of concentration. As the driving force for grain growth $P = \frac{\gamma}{\bar{R}}$, and the Henry adsorption isotherm $\Gamma(c) = Bc$, the relation (18) can be represented as:

$$\frac{\frac{1}{2\bar{R}} - \frac{f}{r}}{c_A} > \frac{1}{2\bar{R}c_0} \tag{19}$$

The volume fraction of the particles $f = \frac{W_p\Omega_p}{W_p\Omega_p + W_{sol.sol.}\Omega_{sol.sol.}}$, where Ω_p and $\Omega_{sol.sol.}$ are the molar volumes of the second-phase particles and the solid solution, respectively. For sake of simplicity we will assume that $\Omega_p \simeq \Omega_{sol.sol.}$. It is pointed out that strictly speaking in the vicinity of the solubility limit the isotherms which take into consideration the interaction between species should be used [10, 13]. We only use the Henry isotherm to make a rough estimate, i.e. to establish the physical link between the parameters of the problem.

Relations (11), (12), and (19) yield:

$$\frac{1 - \frac{2\bar{R}}{r} \cdot \frac{c_0 - c_A}{c_B - c_A}}{c_A} > \frac{1}{c_0} \tag{20}$$

or

$$\frac{2\bar{R}}{r} < \frac{c_B}{c_0} \tag{20a}$$

The relations (20) and (20a) determine the conditions under which the formation of the second-phase particles accelerates grain growth in the alloy. As mentioned previously, the relations (20) and (20a) are derived under the assumption that the second-phase particles are immobile. One can see that the larger r (radius of a particle) and the smaller the mean grain size $\bar{R}$ the more accurate the mentioned relations. For $c_B \sim 1$, $c_0 \sim 10^{-3}$, $c_A \sim 10^{-4}$ the relation 20(a) yields $\frac{2\bar{R}}{r} < 10^3$.

However, the phenomenon discussed might be observed as well in the case when the particles are moving together with the grain boundary, in other words, for small, mobile particles. As noted above, the theory of grain boundary motion dragged by mobile particles was developed in [10, 11].

The physical reason for particle dragging is an attractive force between grain boundary and particle (so-called Zener force and its variants [10]). As shown in [11] the velocity of joint motion of a grain boundary and the particles reads:

$$V = \frac{Pm_b}{1 + \sum_i n_i \frac{m_b}{m_p(r_i)}} \tag{21}$$

where n_i and $m_p(r_i)$ are the number of particles with radius r_i per unit area and the mobility of particles with radius r_i.

For a continuous size distribution of particles $\bar{n}(r)$ we obtain

$$V = \frac{Pm_b}{1 + \int_0^\infty \frac{\bar{n}(r)m_b}{m_p(r)}dr} \tag{22}$$

where $m_p(r)$ is the mobility of a particles with the size $r$and the total number of particles per unit area n

$$n = \int_0^\infty \bar{n}(r)\,dr \tag{23}$$

The border between free grain boundary motion and the joint motion of a grain boundary and the particles is established by dimensionless criterion ρ:

$$\rho = \int_0^\infty \frac{\bar{n}(r)m_b}{m_p(r)}\,dr \tag{24}$$

If $\rho \ll 1$ then $V \cong m_b P$ and the grain boundary velocity is determined by the mobility of the boundary. If $\rho \gg 1$ grain boundary motion is determined by the mobility of the particles and their distribution function:

$$V \cong \frac{P}{\int_0^\infty \frac{\bar{n}(r)}{m_p(r)}\,dr} \tag{25}$$

or in the simple case of a single size distribution:

$$\bar{n}(r) = n_0\delta(r - r_0) \tag{26a}$$

$$V = \frac{Pm_p(r_0)}{n_0} \tag{26b}$$

$$\rho = \frac{n_0 m_b}{m_p(r_0)} \tag{26c}$$

where $n(r_0)$ is the number of particles of size r_0 per unit area.

The particle mobility is determined by it size and mass transport mechanism. If mass transport is conducted through the bulk of a particle, $m_p(r) \sim \frac{1}{r^3}$, if it is operated by interfacial diffusion, $m_p(r) \sim \frac{1}{r^4}$ [10]. In the case, when a particle moves by interfacial diffusion (D_s) transfer, ist mobility is defined by Equation 9.

With the formation of second-phase particles the concentration of the solute solution is reduced while the inherent grain boundary mobility and grain boundary

surface tension increase correspondingly. The surface tension increases in such a process only very moderately. So, the condition of grain growth acceleration can be written (in the case of a single size distribution with the radius r_0) as:

$$V = \frac{Pm_p(r_0)}{n_0} > V(c_0) \tag{27}$$

The volume fraction f of the particles is given by the expression:

$$f = \frac{W_p\Omega_p}{W_p\Omega_p + W_{sol.sol.}\Omega_{sol.sol.}} = \frac{c_0 - c_A}{c_B - c_A} \tag{28}$$

On the other hand, $f = \frac{4}{3}\pi r_0^3 N$, where N is the number of particles per unit volume of the system and

$$N = \frac{3}{4\pi r_0^3} \cdot \frac{c_0 - c_A}{c_B - c_A} \tag{29}$$

It follows that

$$n_0 = 2r_0 N = \frac{3}{2\pi r_0^2} \cdot \frac{c_0 - c_A}{c_B - c_A} \tag{30}$$

From (9) and (27)–(30) we arrive at the condition for grain growth acceleration due to evolving mobile second-phase particles:

$$r_0^2 < \Omega_a \delta \Gamma(c_0) \frac{D_S}{D_{im}} \cdot \frac{c_B - c_A}{c_0 - c_A} \tag{31}$$

We remind that the concentration dependence of grain boundary velocity (or grain growth rate) was estimated in the Lücke-Detert approximation. For

$$D_S \approx 10^{-10}\,\mathrm{m^2 s^{-1}},\ D_{im} \approx 10^{-14}\,\mathrm{m^2 \cdot s^{-1}},$$
$$\Omega_a \approx 10^{-5}\,\mathrm{m^3 \cdot mol^{-1}},$$
$$\Gamma(c_0) \approx 10^{-5}\,\mathrm{mol \cdot m^{-2}},\ \delta \approx 10^{-9}\,\mathrm{m},$$
$$c_B \approx 1,\ c_A \approx 10^{-4},\ c_0 \simeq 10^{-3}$$

we obtain $r_0 < 10^{-6}$ m.

Grain boundary motion together with the particles is bound to have a point of a detachment. As mentioned above the limiting velocity of grain boundary motion together with the particles is described by Equation 12 while the detachment condition can be represented as:

$$f(r_0)m_p(r_0) < V(c_A) \tag{32}$$

or, using for $f(r)$ the relation derived in [14] $f(r_0) = \frac{3}{2}\pi\gamma_b r_0$ and for $m_p(r_0)$ Equation 9:

$$\frac{r_0^3}{\bar{R}} > \delta\Omega_a\Gamma(c_A)\frac{D_S}{D_{im}} \tag{33}$$

One can see that for the values of the parameters given above the relation (33) is obeyed for

$\frac{r_0^3}{\bar{R}} > 10^{-15}\,\mathrm{m^2}$, for instance, by $r_0 > 10^{-7}$ m and $\bar{R} < 10^{-6}$ m.

Consequently, the predicted effect can be observed in systems with mobile and immobile particles. From Equations 20 and 20a follows that in samples with immobile particles systems with low solute solubility (c_A and c_0 are small) and rather small mean grain size $\bar{R}$ are more amenable to observe the effect, while for mobile particles the main condition relates to the size of the particles: they must be sufficiently small.

Evidently, the necessary conditions to discover the effect of Particle Accelerated Grain Boundary Migration or Particle Accelerated Grain Growth—are not so tough. The determination of such conditions is one main goal of GBE.

An important parameter of the Equations 20–33 is the size r of the precipitates. It relates to the solution of a classical problem—the size of an equilibrium nucleus in a solid. Consequently, the change of free energy of the system due to precipitation is considered as the sum of:

1. Bulk free energy ΔG_{bulk}: $\frac{4}{3}\pi r^3(g_2 - g_1)$ where g_1 and g_2 are the free energy per unit volume for matrix and new phase respectively. For $g_2 < g_1$ this term is negative.
2. Surface free energy of the nuclei ΔG_{surf}: $4\pi r^2\gamma_{int}$ (γ_{int} is the surface tension between the nucleus and matrix phase). This term is positive.
3. The elastic free energy (ΔG_{el}) which results from the difference in atomic volume of the phases. This term is positive.

However the formation of equilibrium nuclei requires an equilibrium over all parameters, including the vacancy concentration. In other words, in the volume where a spherical (for the sake of simplicity) nuclei is formed the initial concentration of vacancies c^{eq} should be changed to the value $c^{eq}\exp(\frac{\gamma_{int}\Omega_a}{rkT})$, in accord with the Gibbs-Thomson equation. This, in turn, implies a change of the free energy of the system:

$$\Delta G'_{vac} = \frac{1}{2} \cdot \frac{NkT}{c^{eq}_{matrix}} \left[c^{eq}_{matrix} - c^{eq}_{matrix} \exp\left(\frac{\gamma_{int}\Omega_a}{rkT}\right)\right]^2 \cdot V' \tag{34}$$

where c^{eq}_{matrix} is the equilibrium vacancy concentration in the matrix phase, V' is the volume per nucleus.

The vacancy concentration in a spherical nucleus must be lower than the vacancy concentration in an infinite bulk. However, all phase diagrams relate to equilibrium with a flat surface. By this is meant that defining the free energy of the nuclei we should either take into account a curvature dependence of g_2, or to add the term which takes into consideration the vacancy free

energy of a nucleus with the curved surface:

$$\Delta G''_{\text{vac}} = \frac{1}{2} \cdot \frac{NkT}{c^{\text{eq}}_{\text{nuc}}} \left[c^{\text{eq}}_{\text{nuc}} \exp\left(-\frac{\gamma_{\text{int}} \Omega_{\text{a}}}{rkT} \right) - c^{\text{eq}}_{\text{nuc}} \right]^2 \times \frac{4}{3} \pi r^3 \tag{35}$$

$c^{\text{eq}}_{\text{nuc}}$ is the equilibrium vacancy concentration in the nucleus phase with a flat surface. The critical radius of a nucleus can be defined from an equation which takes into consideration all mentioned terms:

$$\frac{d\Delta G}{dr} = \frac{d}{dr} \Sigma(\Delta G_{\text{bulk}}, \Delta G_{\text{int}}, \Delta G_{\text{el}}, \Delta G_{\text{vac}}) = 0 \tag{36}$$

Accounting for the vacancy contribution to the nucleus free energy Equations 38 and 39 increases the size of equilibrium nucleus. This is understandable: both contributions given by the mentioned equations increase the value of g_2, i.e. reduce the gain in free energy due to the nucleus formation.

It is natural to expect that elastic stresses appear during a first order phase transition. The question is whether it is necessary to take into account this effect in thermodynamic consideration. Are elastic stresses compatible with the thermodynamic equilibrium of a system? A system left to its own devices will find a way to eliminate the elastic stresses—up-hill diffusion, Nabarro-Herring and Coble creep. In this sense the stresses in a crystal are incompatible with complete equilibrium. However, at low temperatures the rate of relaxation processes, diffusion for instance, is rather small, and the term ΔG_{el} should be included in the free energy of nucleus formation.

5. Kinetics of grain growth inhibited by vacancy generation

Even a crystal of a pure element has its intrinsic impurities—the vacancies. It is a rather elaborate problem to account for the effect of vacancies on the processes in solids. Vacancies do not only influence the kinetics of the processes in solids but the thermodynamics as well. The point is that the excess of grain boundary free volume produced by the reduction of total area of grain boundaries (the density of grain boundaries is smaller than the density of an ideal crystal) can be considered as a flux of vacancies into the bulk of a sample, as a source of elastic stresses, as a source of plastic deformation. However, in principle the approach which considers the elimination of volume excess by the vacancies is most constructive. Actually, the way to reduce the excess through elastic stresses is a deadlock. The relaxation of elastic stresses is a long term and slow process, that is why in a short time the reduction of grain boundary area will result in a strong increase of free energy. Moreover, as mentioned above, the relaxation of elastic stresses occurs by a directed flux of vacancies. The inhibiting effect of vacancies on the very process in which they are generated is considered from a thermodynamic viewpoint in [15–19]. It is very common in materials science that vacancies are generated as a by-product of a kinetic process. Vacancy production by moving jogs on dislocations during plastic deformation, by a progressing solid/liquid interface in solidification, or, generally, in every first order phase transition, or by shrinking voids in sintering, or, finally, during grain growth due to the different density of grain boundary and the ideal crystal [20–22], are but a few examples. The excess free volume the system has to get rid of in such kinetic processes is released as vacancies which have to be accommodated by the crystal bulk. A vacancy is an "impurity atom" which is solved in any crystal, and the distinctive property of which (comparing with ordinary impurities) is that a vacancy is born from vacuum and disappears in vacuum, i.e. there is no conservation rule. Other than that the properties of vacancies are similar to usual impurities: creating a solution even in absolutely pure crystals vacancies decrease its free energy; if the vacancy concentration exceeds the solubility limit—the equilibrium concentration of vacancies c^{eq}—they try to leave the crystal or to precipitate as second-phase particles—i.e. voids. The kinetic aspect of vacancy influence on grain growth was considered yet [23, 24]. In [19, 22] it was shown that in the course of grain growth a self-dragging by the fission product of grain boundaries can be observed.

In most general terms, the Gibbs free energy G of a system with vacancies can be written as

$$G = G_{\text{non-vac}} + G_{\text{vac}} \tag{37}$$

where $G_{\text{non-vac}}$ is the non-vacancy part of the Gibbs free energy and G_{vac} is the contribution due to vacancies. Obviously small deviations of the vacancy concentration c from its equilibrium value c^{eq} should increase the last term in (37) irrespectively of a sign of the difference $c - c^{\text{eq}}$:

$$G_{\text{vac}} = \frac{1}{2} \frac{NkT}{c^{\text{eq}}} (c - c^{\text{eq}})^2 \tag{38}$$

Here N is the number of atomic sites per unit volume.

The grain growth process is driven by the tendency of the system of grain boundaries to reduce the total grain boundary energy (grain boundary area if all grain boundaries are assumed to be equal in their propreties (uniform grain boundary model).

As a 'by-product' of this process, vacancies are released into the crystal bulk. Indeed, according to the present views the density of a grain boundary is lower than that of the bulk. The excess free volume released during the reduction of the grain boundary 'phase' has to be accommodated by the bulk. This assumption is supported by recent computer simulations of grain boundary motion [22]. The supply of vacancies by moving grain boundaries may produce a vacancy supersaturation in the bulk rising the Gibbs free energy and producing a thermodynamic force on the boundary. As can be expected intuitively, particularly by analogy with the Le Chatelier principle, this thermodynamic force will resist grain boundary migration. Under certain conditions considered in [15–17], this effect may

be as strong as to temporarily suppress grain growth altogether. In the approach proposed uninhibited grain growth was cosidered to occur only during a limited time t^* Equation 39. It was assumed that after that time, on reaching the condition when the time derivative of the free energy of the system becomes positive, "locking" of grain growth occurs:

$$t \geq t^* = \frac{1}{24} \cdot \frac{\gamma c^{\mathrm{eq}} R^2}{NkT(\beta\delta)^2 V} \tag{39}$$

Here V is the "unperturbed" rate of grain growth driven by the boundary energy; γ, δ, β and m are grain boundary characteristics: free energy per unit area, thickness, the relative excess free volume, and mobility, respectively; $\bar{R}$ is the average grain size (radius), D_{SD} is the bulk self-diffusion coefficient, N is the number of atoms per unit volume and Z is the coordination number; kT has its usual meaning. Under the assumpion that $t^* \ll \tau = d^2/D_{\mathrm{v}}$ the expression for the effective velocity of grain growth V_{eff} can be written as

$$V_{\mathrm{eff}} = \frac{t^*}{\tau} V = \frac{1}{24} \cdot \frac{\gamma D_{\mathrm{SD}}}{NkTZ(\beta\delta)^2} \tag{40}$$

Smoothing the discontinuous solution by replacing V_{eff} with the time derivative of the average grain size, *dR/dt,* and solving Equation 39 yields the time law for the grain growth model of [15, 17]:

$$\frac{1}{\bar{R}_0} - \frac{1}{\bar{R}} = \frac{1}{24} \cdot \frac{\gamma D_{\mathrm{SD}} t}{NkTZ(\delta\beta)^2 d^2} \tag{41}$$

where $\bar{R}_0$ is the initial grain size.

The model picture outlined above appears to account for the inhibiting effect of vacancies on grain growth, but, of course, it is not more than an approximation of the real continuous process of grain growth. Guided by the principle that *natura non facit saltus*, the authors of [18, 19] suggested a description of grain growth as a continuous process.

An equation expressing the balance of energy associated with an increment of grain size, *dR* within a time increment *dt* can be written as:

$$-\frac{d}{d\bar{R}}\left(\frac{3\gamma}{2\bar{R}}\right) d\bar{R} = \frac{3}{2} \cdot \frac{1}{\bar{R}} \frac{(d\bar{R}/dt)^2}{m_{\mathrm{b}}} dt + \frac{NkT}{c^{\mathrm{eq}}}(c - c^{\mathrm{eq}}) \frac{6\beta\delta}{\bar{R}^2} d\bar{R} \tag{42}$$

Left hand side of (42) is distributed between the dissipation due to the drag forces (first term in the right hand side of Equation 42 and the vacancy sub-system (second term in the right hand side of Equation 42. The variation of the vacancy concentration is given by

$$\dot{c} = \frac{6\beta\delta}{\bar{R}^2} \cdot \frac{d\bar{R}}{dt} - \frac{D_{\mathrm{v}}}{d^2}(c - c^{\mathrm{eq}}) \tag{43}$$

Here d and D_{v} are the average spacing between vacancy sinks and the vacancy iffusivity correspondingly. The ratio $\frac{d^2}{D_{\mathrm{v}}}$ determines the characteristic vacancy annihilation time. Equations 42 and 43 give us a full description of the evolution of the grain system in terms of the average grain radius and the vacancy concentration and in a dimensionless form they can be re-written as:

$$\xi \frac{d\xi}{dt} + A\Psi C - A = 0 \tag{44}$$

$$\frac{dC}{dt} = \frac{p}{\xi^2} \frac{d\xi}{dt} - C \tag{45}$$

Here $\xi = \bar{R}/d$, $C = c - c^{\mathrm{eq}}$, $A = m_{\mathrm{b}}\gamma/D_{\mathrm{v}}$, $\Psi = \frac{4NkT(\delta\beta)}{c^{\mathrm{eq}}\gamma}$, $p = 6\beta\frac{\delta}{d}$; the time t is now non-dimensional and is measured in the units of d^2/D_{v}.

Numerical solutions of the above set of equations for a broad range of parameters has shown that for sufficiently small initial grain size $\xi_0 = R_0/d$ the grain growth uninhibited by vacancies is preceded by an incubation time during which the growth rate is substantially reduced, the time dependence of the grain size exhibiting a plateau-like behaviour, cf. Fig. 2a. For large values of ξ_0 no incubation time is observed. The incubation time is defined as the time at which the grain growth rate is a maximum. This time corresponds to the termination of the plateau-like behaviour and a transition to uninhibited, parabolic grain growth, cf. Fig. 2a. Over the incubation time, the vacancy concentration stays at an approximately constant, increased level, cf. Fig. 2b.

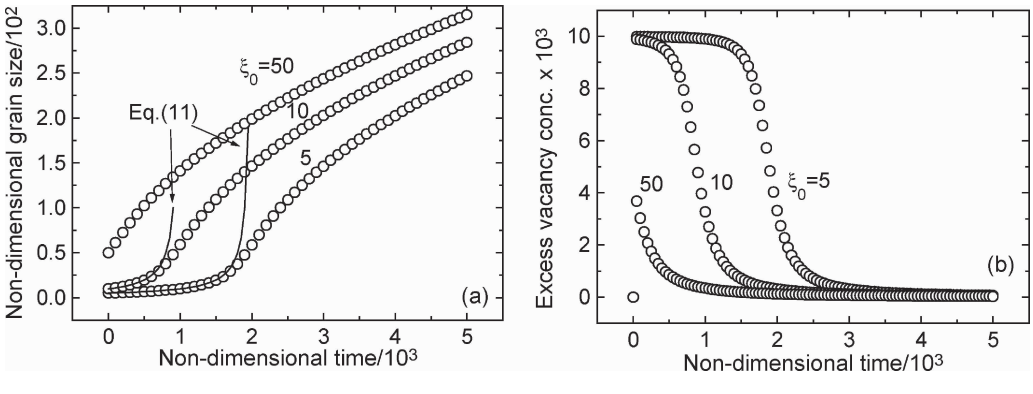

Figure 2 Dependence of non-dimensional grain size (a) and of excess vacancy concentration (b) on the non-dimensional time calculated from Equations 44 and 45 for the following values of parameters: $A = 10$, $\Psi = 100$ and $p = 100$ [18].

Numerical results show that the non-dimensional incubation time is inversely proportional to ξ_0 and can be represented by the following formula:

$$\tau_{\text{incubation}} = \frac{p\Psi}{\xi_o} \tag{46}$$

or, in dimensional form:

$$t_{\text{incubation}} = 24\frac{NkT(\beta\delta d)^2}{\gamma \bar{R}_0 D_{\text{SD}}} \tag{47}$$

where D_{SD} is the bulk self-diffusion coefficient.

For times larger than the incubation time, a common parabolic grain growth law follows, while within the incubation time an approximate analytical solution of the set of Equations 46 and 47 reads:

$$C = 1/\Psi \tag{48}$$

$$\frac{1}{\xi_o} - \frac{1}{\xi} = \frac{t}{p\Psi} \tag{49}$$

which, being rewritten in the dimensional form, reads:

$$\frac{1}{\bar{R}_0} - \frac{1}{\bar{R}} = \frac{1}{24} \cdot \frac{\gamma D_{\text{SD}} t}{NkT(\beta\delta)^2 d^2} \tag{50}$$

This demonstrates that the approximation [15, 16] based on the intermittent locking-unlocking scheme with smoothing, provides a quantitatively adequate representation of continuous grain growth in the regime where the inhibiting effect of grain growth induced vacancies is operative. Indeed, Fig. 2 demonstrates an excellent match between the $\xi(t)$ dependencies over the incubation period given by Equations 49 and 50.

The condition for the occurrence of the vacancy-induced stabilization against grain growth can be extracted from a comparison of the inhibited grain growth with the common, parabolic grain growth. Actually, parabolic growth occurs if the vacancy effect can be neglected, i.e. if the vacancy concentration is sufficiently close to its equilibrium value. From Equation 44 it then follows

$$\xi^2 - \xi_o^2 = 2At \tag{51}$$

Obviously, the solution of the set of Equations 44 and 45 coincides with the parabolic law given by Equation 51 for time tensing to zero and also for times much larger than the incubation time, when C tends to zero, cf. Fig. 2. A real inhibition of grain growth means that the rate of growth in the plateau region, described by Equation 49, is much smaller than that corresponding to 'free', uninhibited growth described by Equation 51. This condition reads

$$\xi \ll (Ap\Psi)^{1/3} \tag{52}$$

or in the dimensional form:

$$\bar{R}_0 \ll \bar{R}_c^* = \left[24NkTZ(\delta\beta)^2 d^2 \frac{m_b}{D_{\text{SD}}}\right]^{1/3} \tag{53}$$

One can see that this condition is not very material sensitive, particularly due to the fact that the ratio of the grain boundary mobility and the coefficient of bulk self-diffusion is not strongly material dependent, and also due to the power of 1/3. One possible source of structural dependence is the sink spacing d, for example if it is related to the inverse of the square root of the dislocation density may bring about some variability of the quantity on the right hand-side of inequality (Equation 53).

One particular case needs to be considered separately, though. It is the case when the initial grain size is so small that no other vacancy sinks but the grain boundaries themselves are available, so that d is to be identified with the grain size $\bar{R}$. Equation 50 then changes to

$$\frac{dC}{dt} = \frac{1}{\xi^2}\left(6\frac{d\xi}{dt} - C\right) \tag{54}$$

Equation 49 remains unchanged. However, the meaning of the non-dimensional grain size and the non-dimensional time are different now: $\xi = \bar{R}/(\delta\beta)$, and time is measured in units of $(\delta\beta)^2/D_v$.

Solving the set of Equations 49 and 54 numerically, one can see that the temporal behaviour of the grain size in this case is different from the behaviour in the case of constant sink spacing d. After a short initial period of time t_{trans} the rate of vacancy-inhibited growth slows down considerably (Fig. 3a). After that, the grain growth effectively stays inhibited for very long times. The growth rate is thus always lower than the respective rate of usual parabolic growth (Fig. 3b). Again, using the fact that after the transient period t_{trans} the vacancy concentration is sustained at an approximately constant level and that the grain size does not change significantly, we arrive at an approximate solution of the set of Equations 49 and 54 which reads

$$\bar{R} - \bar{R}_0 = \frac{1}{24} \cdot \frac{\gamma D_{\text{SD}} t}{NkTZ(\delta\beta)^2} \tag{55}$$

From Fig. 3b one can see that Equation 54 provides indeed a good analytical approximation for sufficiently short times, which neverthekess should be longer than t_{trans}.

The stability condition of nanocrystalline material against grain growth can be expressed by the inequality

$$\bar{R}_0 \ll \bar{R}_c = 24NkTZ(\delta\beta)^2 \frac{m_b}{D_{\text{SD}}} \tag{56}$$

These results have an interesting interpretation: a nanocrystalline material cannot be stable if condition (56) or (53) (whichever is relevant) is violated. In that sense, the critical radius $\bar{R}_c$ or $\bar{R}_c^*$ can be regarded as a limiting stable grain size above which grain growth uninhibited by vacancies is possible. Obviously, as seen from (53) and (56) the critical grain size is temperature dependent. As the activation energies for grain boundary mobility and the self-diffusion are generally different [10], the sense of the temperature variation of the critical grain size will depend on the interplay of

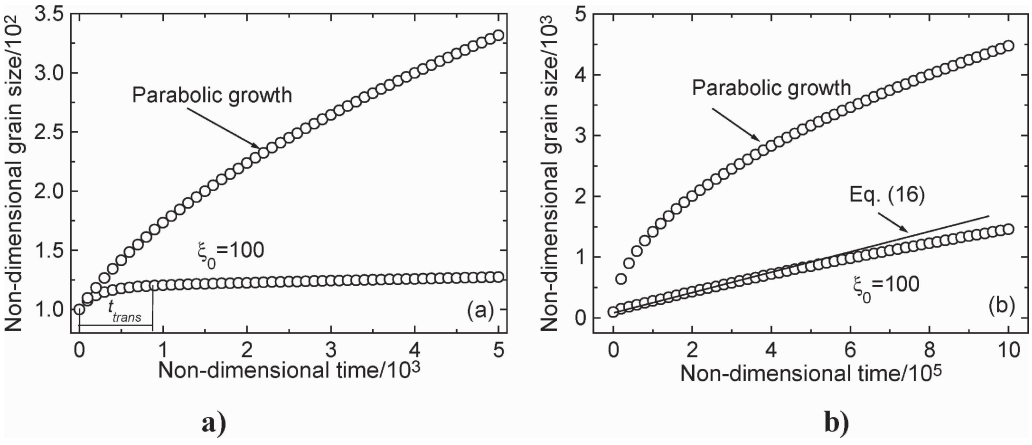

Figure 3 Dependence of non-dimensional grain size on the non-dimensional time calculated from Equations 44 and 54 for the following values of parameters: $A = 10$, $\Psi = 100$ for two different time scales [18].

the temperature dependencies of the mobility and the self-diffusion coefficient. It should be stressed that the grain boundary mobility may depend very strongly on the type of the boundary, the texture in the material and its purity [10], which makes estimation of the critical radius to a fairly difficult task. In [18] such an estimation was done for Al—the only material for which m is known with some confidence—at 300°C one obtains both $\bar{R}_c$ and $\bar{R}_c^* = (\bar{R}_c d^2)^{1/3}$of the order of 100 nm. These estimates can, from our viewpoint, explain the relative stability of nanocrystalline materials against grain growth.

The results of the described approach were compared with grain growth experiments in nanocrystalline Fe [25]. As intimated by the authors of [25] the theory developed is able to account for the growth-rate discrepancy between nanocrystalline and microcrystalline Fe without recourse to impurity effects.

In the following we discuss aspects of the present kinetic description of the interaction between the process of grain growth and the evolution of the vacancy sub-system. The set of Equations 49 and 50, or 49 and 54, admits solutions corresponding to a decrease of the average grain size for the case of an initial vacancy supersaturation. In other words, it can be speculated that grain refinement can be induced by high vacancy concentration, which can be created in different ways, e.g. by quenching from a high temperature, irradiation with energetic particles or plastic deformation. An example of the computed variation of the average grain size with time for three different initial excess vacancy concentrations is shown in Fig. 4. While the amount of grain size decrease is small, the very possibility of vacancy-induced grain refinement appears interesting.

The physical reason for this grain refinement is similar to the well known effect of grain refinement during discontinuous precipitation (DP) [26], diffusion induced grain boundary migration (DIGM) [27] and discontinuous ordering (DO) [28] reactions. In all cases the loss of energy associated with an increase of grain boundary area is compensated for by the energy gain in the bulk due to decomposition of supersaturated solution (DP), formation of the solid solution (DIGM) or bulk ordering of the quenched disordered alloy (DO) behind moving grain boundaries.

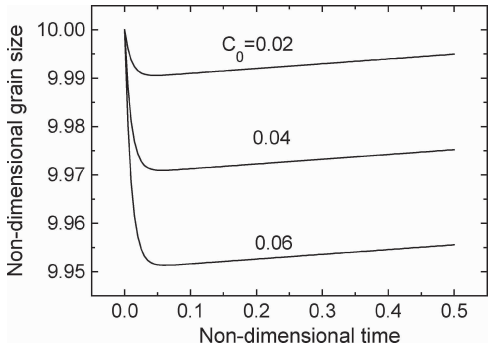

Figure 4 Dependence of non-dimensional grain size on the non-dimensional time calculated from Equations 44 and 45 for various levels of initial vacancy supersaturation. (Parameter values are the same as in Fig. 2) [18].

The discussed approach was applied to grain growth in thin films, one of the most important subjects of modern high technologies. Grain growth in thin films has some distinctive properties, which are mainly connected with the stresses developing in thin films and with a strong influence of the free surface on grain boundary motion [29, 30]. The consideration of the first feature dates back to Chaudhari [31]. First, the cohesion between a film and a substrate should lead to internal stresses in the film. Second, under certain conditions, an equilibrium grain size can exist beyond which no grain growth occurs. This latter result followed from a consideration of an interplay between the elastic strain energy and the total grain boundary energy during grain growth. The model proposed by Chaudhari appears to be commonly accepted, see, e.g., a recent review [32]. In that approach, it was tacitly assumed that the excess free volume of grain boundaries released during grain growth disappears instantly, giving rise to a tensile stress. This strong assumption limits the applicability of the model, as the free volume release would normally occur via generation of lattice defects, notably the injection of vacancies into the bulk of the material [22].

In accordance with [31] the stress in thin film is given by

$$\sigma = \frac{E}{(1-\nu)}\left\{\frac{1}{2}\beta\delta\left(\frac{1}{R_0}-\frac{1}{R}\right)-\alpha(c-c^{\mathrm{eq}})\right\} \quad (57)$$

Here $E/(1-\nu)$ is the biaxial elastic modulus expressed in terms of Young's modulus E and Poisson's ratio ν.

As it was mentioned above, Chaudhari's approximation presumes that the excess volume disappears instanteneously, while in our approach part of it is contained in the vacancies. In this case the resulting stress can be expressed by

$$\sigma = \frac{E}{2(1-\nu)}\left\{\beta\delta\left(\frac{1}{R_0}-\frac{1}{R}\right)-(c-c^{\mathrm{eq}})\right\} \quad (58)$$

Consider the derivative of the full Gibbs free energy, $G = G_{\mathrm{s}} + G_{\mathrm{GB}} + G_{\mathrm{vac}}$, with respect to the average grain size R:

$$\frac{dG}{dR} = \left[\frac{NkT}{c^{\mathrm{eq}}}(c-c^{\mathrm{eq}})-\frac{\sigma}{2}\right]\cdot\frac{dc}{dR}+\left\{\frac{1}{4}\frac{E}{1-\nu}\beta\delta \times\left[\beta\delta\left(\frac{1}{R_0}-\frac{1}{R}\right)-(c-c^{\mathrm{eq}})\right]-\gamma\right\}\frac{1}{R^2} \quad (59)$$

The behaviour of the system can be diagnosed by an analysis of the sign of this derivative. The thermodynamic viability of the grain growth process requires that the derivative be negative.

The evolution of the vacancy concentration with time t is given by

$$\frac{dc}{dt} = \frac{\beta\delta}{R^2}V - \frac{D_{\mathrm{v}}}{d^2}(c-c^{\mathrm{eq}}) \quad (60)$$

The first term on the right-hand side represents the rate of vacancy generation accompanying grain growth (V being the grain growth rate, or the velocity of grain boundary migration). The second term describes the vacancy removal by diffusion to the film surface, D_{v} being the vacancy diffusivity an d the film thickness.

Two essentially different situations of grain growth in thin films can be considered.

When vacancy removal can be neglected (which can be referred to as the 'adiabatic' case) $\sigma = 0$ and the last term in (60) can be dropped leading to

$$\frac{dc}{d\bar{R}} = \frac{\beta\delta}{\bar{R}^2} \quad (61)$$

Equation 59 then assumes the form

$$\frac{dG}{d\bar{R}} = \frac{1}{\bar{R}^2}\left\{-\gamma+(\beta\delta)^2\frac{NkT}{c^{\mathrm{eq}}}\left(\frac{1}{\bar{R}_0}-\frac{1}{\bar{R}}\right)\right\} \quad (62)$$

It is seen that in the early stages of grain growth, when $\bar{R}$ is close to $\bar{R}_0$, the derivative $dG/d\bar{R}$ is negative, meaning that the process is favourable thermodynamically. However, at a certain critical value of $\bar{R}$ given by

$$\bar{R}_0 = \frac{\bar{R}_0}{1-\frac{\gamma c^{\mathrm{eq}}\bar{R}_0}{(\beta\delta)^2 NkT}} \quad (63)$$

the derivative $dG/d\bar{R}$ vanishes. This critical value of R can be seen as an 'equilibrium' grain size beyond which no growth will occur. Obviously, such a critical grain size is only possible if the denominator of Equation 63 is positive, i.e. if

$$\bar{R}_0 < \frac{(\beta\delta)^2 NkT}{\gamma c^{\mathrm{eq}}} \quad (64)$$

A simple estimate using representative values of the parameters,

$$\delta = 10^{-9}\,\mathrm{m}, \quad \beta = 2\cdot 10^{-2}, \quad \gamma = 1\,\mathrm{J}\cdot\mathrm{m}^{-2},$$
$$T = 500\,\mathrm{K}, \quad c^{\mathrm{eq}} = 10^{-8},$$

shows that this condition is fulfilled for $\bar{R}_0 < 1.5\cdot 10^{-5}$ m. Of course, this value is strongly temperature dependent, primarily through the thermal equilibrium vacancy concentration. If inequality (64) is not fulfilled, grain growth will be unrestricted.

The second situation, which can be called as the 'Chaudhari' Approximation [31], also follows from Equations 60 and 61. Indeed, assuming the existence of such a critical radius and thus setting V to zero and further assuming that the vacancy concentration is equal to its thermal equilibrium value (a tacit assumption in Chaudhari's paper [31]) we find that

$dG/d\bar{R} = 0$ if

$$\bar{R} \cong \frac{\bar{R}_0}{1-\frac{4\gamma\bar{R}_0(1-\nu)}{E(\beta\delta)^2}} \quad (65)$$

This formula reproduces Chaudhari's result [31], which was recently revisited by Thompson and Carel [32].

The modified energy balance equation reads:

$$\frac{\gamma}{\bar{R}^2}\frac{d\bar{R}}{dt} = (1-\nu)\frac{\sigma}{E}\frac{d\sigma}{dt} + \frac{NkT}{c^{\mathrm{eq}}}(c-c^{\mathrm{eq}})\frac{\beta\delta}{\bar{R}^2}\frac{d\bar{R}}{dt}+\frac{V^2}{m\bar{R}} \quad (66)$$

The set of Equations 66 and 61, with σ given by Equation 57, provide a full description of the time evolution of the grain size, vacancy concentration and stress. The numerical solution manifests the features very similar to those for the bulk and shows that—despite the two factors inhibiting grain growth, *viz.* the development of elastic strain and of vacancy supersaturation accompanying the loss of grain boundary area—grain growth occurs at all conditions. In other words, there is no critical initial grain radius $\bar{R}_0$ below which grain growth would be limited, contrary to the prediction in [31]. However, in a range of parameters of practical importance, the temporal behaviour of a polycrystalline thin film may exhibit an incubation period during which the grain size changes by only a small fraction of its initial value. It is in that sense that one can refer to the incubation time as a period of stability of grain structure. The magnitude of the incubation time is given by Equation 67 which provides a tool for assessing the period of stability of a thin film of a given thickness against grain

growth for a temperature of interest.

$$t^{*}_{\text{incubation}} = \frac{(\beta\delta)^2 NkT}{\gamma \bar{R}_0} \cdot \frac{d^2}{D_{\text{SD}} c^{\text{eq}}} \tag{67}$$

This makes it possible to clearly identify the incubation time. Its significance can be interpreted as follows. Even though grain growth does occur during the incubation time, the magnitude of the grain size does not change substantially. For all practical purposes once can thus consider $t_{\text{incubation}}$ as the time of relative stability of the grain structure. Knowing the dependence of $t_{\text{incubation}}$ on the initial grain size, temperature and film thickness, one can assess this time for a system of interest. An interesting feature of the incubation period is that, in addition to the relative stability of grain structure, stability of the vacancy concentration at a high level ($c \cong \frac{NkT\beta\delta}{c^{\text{eq}}\gamma}$) is maintained.

Finally, we note that the Chaudhari case [31] can be construed if a fairly artificial condition is used that the vacancy concentration c is identical to the thermal equilibrium value c^{eq}. What is more, even in a "pure" Chaudhari model there is no complete freeze of grain growth: the elastic stresses generated in the course of grain growth of the thin film generate vacancy fluxes to reduce the stresses, what is very similar to the situations described by Nabarro-Herring and Coble.

From the results considered above it may be deduced that the redistribution of the excess volume in the form of vacancies generated in the course of grain growth stabilizes grain microstructure against coarsening. Some theoretical predictions were confirmed experimentally [25], however much more experimental work is needed to clear up features of the self-inhibited grain growth.

6. Grain boundary triple junctions and their role in grain microstructure evolution

A distinctive property of fine grained and nanocrystalline materials along with the high density of grain boundaries, particles and characteristic behavior of impurities is the extremely high concentration of grain boundary triple junctions. We reason that it is timely to consider the grain growth in fine grained and nanocrystalline materials also with regard to grain boundary triple junctions besides the traditional elements of the process—the grain boundaries.

Although the number of triple junctions in polycrystals is comparable in magnitude with the number of boundaries, all peculiarities in the behaviour of polycrystals during grain growth were solely attributed to the motion of grain boundaries so far. It was tacitly assumed in theoretical approaches, computer simulations and interpretation of experimental results that triple junctions do not disturb grain boundary motion and that their role in grain growth is reduced to preserve the thermodynamically prescribed equilibrium angles at the lines (or the points for 2D systems) where boundaries meet. The most prominent example of how this assumption determines the fundamental concepts of grain structure evolution gives the Von Neumann-Mullins relation, which defines the rate of change of the grain area in the course of grain growth. No doubt this relation forms the basis for practically all theoretical and experimental investigations as well as computer simulations of microstructure evolution in 2D polycrystals in the course of grain growth [33–36]. This relation is based on three fundamental assumptions, namely:

1. all grain boundaries possess equal mobilities (m_{b}) and surface tensions (γ) irrespective of their misorientation and the crystallographic orientations of the boundaries;
2. the mobility of a grain boundary is independent of its velocity;
3. the triple junctions do not affect grain boundary motion; therefore, the contact angles at triple junctions are always in equilibrium and, due to the first assumption, are equal to 120° [37, 38].

Let us consider a $2D$ grain with an area S (Fig. 5). In the time interval dt all points on the grain boundaries of the considered grain will displace normal to the grain boundaries by the amount Vdt, where V is the grain boundary migration rate. Accordingly, the rate of change of the grain area S can be expressed by

$$\frac{dS}{dt} = -\oint V dl \tag{68}$$

where dl is an element of the grain perimeter. For grain growth

$$V = \gamma m_{\text{b}} K \equiv A_{\text{b}} K \tag{69}$$

where m_{b} is the grain boundary mobility, γ is the grain boundary surface tension, K is the local curvature of the grain boundary

$$K = \frac{d\varphi}{dl} \tag{70}$$

where φ is the tangential angle at any given point of the grain boundary.

From from Equations 68–70 follows

$$\frac{dS}{dt} = -A_{\text{b}} \oint d\varphi \tag{71}$$

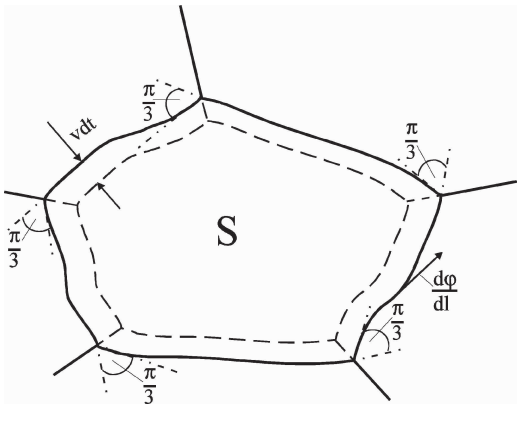

Figure 5 Definition of parameters for the effect of triple junctions for a calculation of the rate of grain area change.

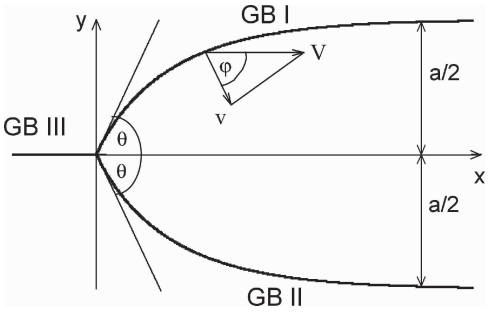

Figure 6 Configuration of grain boundaries at a triple junction during steady state motion for $n < 6$ [10, 41].

If the grain were bordered by a smooth line, the integral in Equation 71 would equal 2π. However, owing to the discontinuous angular change at every triple junction, the angular interval $\Delta\varphi = \pi/3$ is subtracted from the total value 2π for each triple junction. Consequently

$$\frac{dS}{dt} = -A_b\left(2\pi - \frac{n\pi}{3}\right) = \frac{A_b\pi}{3}(n-6) \qquad (72)$$

where n is the number of triple junctions for each respective grain, i.e. the topological class of the grain. Thus, the rate of area change is independent of the shape of the boundaries and determined by the topological class n only. Grains with $n > 6$ will grow and those with $n < 6$ will disappear.

While the first assumption of the derivation agrees with the so-called uniform boundary model, and there is an intuitive feeling that such a grain boundary can be realized, at least, in a "Gedankenexperiment", and the second assumption fits the principles of the absolute reaction rate theory, the third hypothesis should be checked experimentally.

This brings up the question: How to measure the triple junction mobility? There are two possible ways to measure the triple junction mobility. Similar to grain boundaries, reliable data of triple junction mobility can be obtained only in the course of steady-state motion. However a steady-state motion of a grain boundary system with a triple junction is only possible in a very small set of geometrical configurations. Two of them are shown in Figs 6 and 7 [10, 39, 40].

These special boundary systems were investigated in [10, 39, 40] under three main assumptions. Two of them comply with the assumptions (1) and (2) of the Von Neumann-Mullins consideration, while the third one is determined by Equation 69: the normal grain boundary displacement rate v is proportional to the grain boundary curvature K. As shown in [39, 40], the model grain boundary systems (Figs 6 and 7) can move steadily, and the analysis of their motion permits us to understand the influence of the finite mobility of a triple junction on the migration of grain boundaries.

An important relation which links the steady-state value of the angle θ at the vertex of a triple junction with the dimensionless criterion $\Lambda = m_{Tj}a/m_b$ for the configuration represented in Fig. 6 was derived [10, 39]:

$$\frac{2\Theta}{2\cos\Theta - 1} = \frac{m_{Tj}a}{m_b} = \Lambda \qquad (73)$$

If a triple junction is mobile and does not drag grain boundary motion, the criterion $\Lambda \gg 1$ and $\theta = \pi/3$ i.e. the equilibrium angular value at a triple junction in the uniform grain boundary model. In contrast, however, when the mobility of the triple junction is relatively low (strictly speaking, when $\Lambda_{Tj}a \ll m_b$) then $\theta \to 0$ (Fig. 8).

As can be seen from Fig. 6, the model configuration correlates to grains in a polycrystal with less than 6 neighbours (adjacent grains), in other words, the topological class of the grain is smaller than 6. The steady state motion of this system can be described by the same system of equations, as the previous one, only with different boundary and initial conditions [39].

The steady state motion of grain boundary configuration outlined in Fig. 7 corresponds to grains with topological class greater than 6 [39, 40]. The criterion Λ, which describes the influence of the triple junction mobility on grain boundary migration now is defined by

$$-\frac{\ln\sin\Theta}{1 - 2\cos\Theta} = \frac{m_{Tj}\,x_0}{m_b} = \Lambda \qquad (74)$$

Obviously, for $\Lambda \gg 1 \gg 1$, when the boundary mobility determines the kinetics of the system the angle θ tends to its equilibrium value ($\pi/3$).

Again, the angle θ changes when a low mobility of the triple junction starts to drag the motion of the boundary system. However, as can be seen from Equation 78 and Fig. 6, in this case the steady state value of the angle θ increases as compared to the equilibrium state. (Otherwise the triple junction would move in the negative direction of the x-axis, increasing the free energy of the system.)

For $\Lambda \ll 1 \ll 1$ the angle θ (Equation 74) tends to approach $\pi/2$. The dependency $\Lambda = \Lambda(\theta)$ for both $n < 6$ and $n > 6$ are shown in Fig. 8.

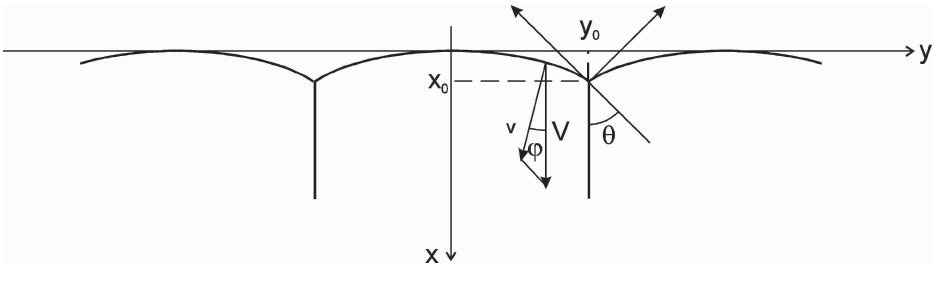

Figure 7 Configuration of grain boundaries at a triple junction during steady state motion for $n > 6$ [39].

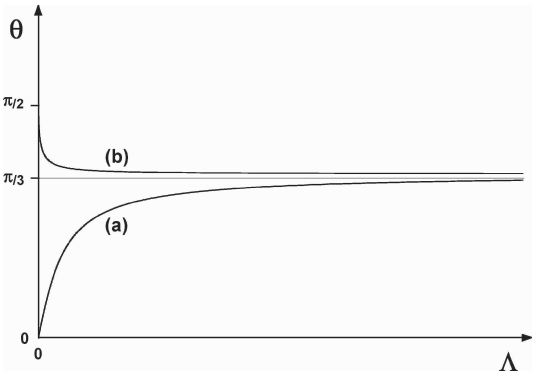

Figure 8 Angle θ as a function of Λ. (a) for $n < 6$, Equation 77; (b) for $n > 6$, Equation 78 [39].

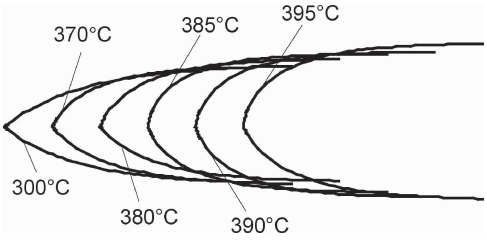

Figure 9 Evolution of the shape of a grain boundary system with triple junction in Zn tricrystals with increasing temperature [41].

It should be stressed that the angle θ is strictly defined by the dimensionless criterion Λ, which, in turn, is a function of not only the ratio of triple junction and grain boundary mobility, but of the grain size as well.

Experimental investigations were carried out for the grain boundary configuration shown in Fig. 6 in specially grown tricrystals of Al and Zn [41, 42]. The motion of different triple junctions formed by high-angle and low-angle boundaries were investigated in the temperature range between 300°C and 410°C (Zn) and 400–600°C (Al). The shape of the moving grain boundary system was similar to the shape predicted by the theory [41]. In particular, it was demonstrated that the vertex angle θ at the triple junction can deviate distinctly from the equilibrium value, when a low mobility of the triple junction hinders the motion of the grain boundaries (Fig. 9). In fact, a transition from triple junction kinetics to grain boundary kinetics was observed (Figs 10 and 11). Experiments revealed that triple junctions do possess a finite mobility. Moreover, the extent of the changes of the angle θ and criterion Λ are such ones that don't permit to explain them by thermodynamic factors and there are no doubts in the kinetic nature of the phenomena.

Molecular dynamics simulation studies of the migration of grain boundaries with triple junctions confirm that the triple junction mobility is finite and can be sufficiently small to limit the rate of grain boundary migration [43, 45]. The major distinctive feature of this study was that molecular dynamics simulations of individual triple junction migration was performed for experimental geometrical configurations shown in Figs 6 and 7 (Figs 12 and 13). The analytical solutions and the analysis of grain boundary motion given in [39–41] serve as a theoretical background of the studies discussed. The static - equilibrium - grain boundary triple junction angles and the dynamic triple junction angles were measured as a function of grain size, grain boundary misorientation and direction of migration. In most cases, the static and dynamic triple junction angles were observed to be nearly identical. However, substantial deviations between the two were observed for low Σ boundary misorientations (Fig. 14). The rate of change of the half-loop grain boundary area during the triple junction migration is compared with that extracted from previously conducted bicrystal simulations, enabling the extraction of intrinsic (albeit normalized) steady-state triple junction mobility [43, 44]. This mobility quantifies the effect of triple junctions on grain boundary migration. Furthermore, the normalized triple junction mobility exhibits strong variations with boundary misorientation, with strong minima at low Σ misorientations. The triple junctions create substantial drag on grain boundary migration at these low mobility misorientations. One interesting feature of the results is that the triple junction mobility depends upon the direction that the triple junction migrates. Again, the normalized triple junction mobility was found to have significant dependence on direction of migration for the case of low Σ grain boundaries (Fig. 14). On the whole, the simulations confirm the experimental observations

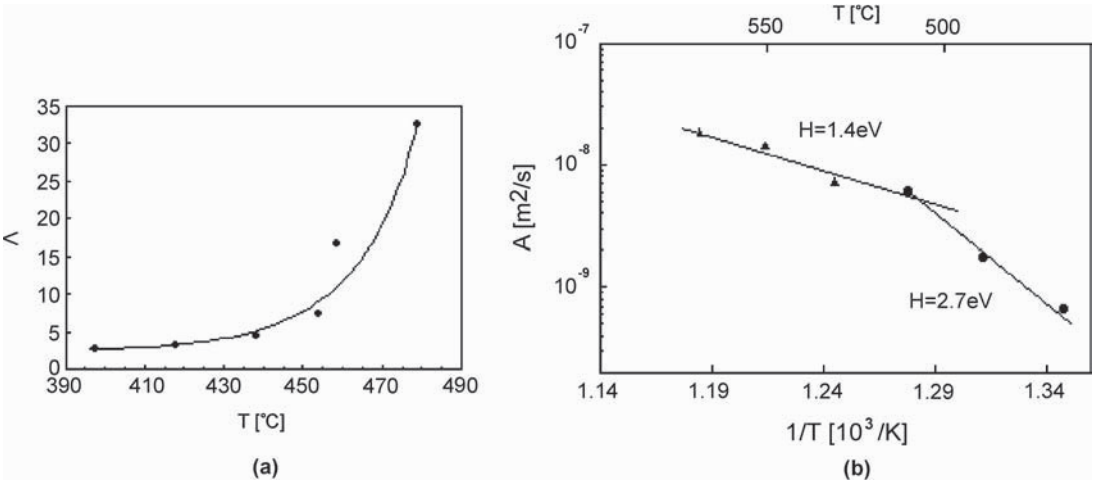

Figure 10 Temperature dependence of the criterion Λ (a) and of triple junction (●) and grain boundary mobility (▲) for $< 111 >$ tilt grain boundary system in pure Al [42].

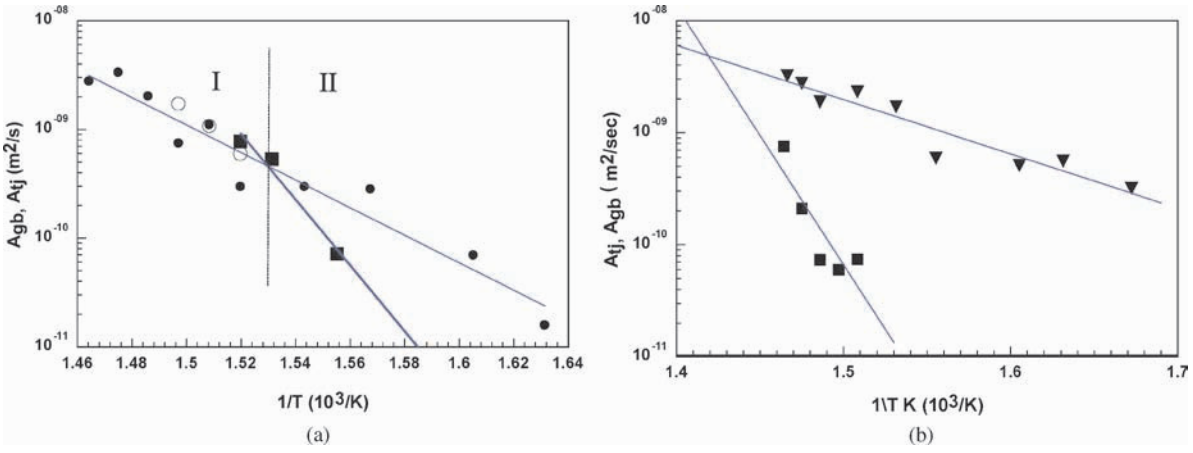

Figure 11 Temperature dependence of reduced grain boundary mobility A_b (solid circles) and reduced triple junction mobility A_{tj} (solid squares) for the system $<10\bar{1}0>$ (a) and for the system $<11\bar{2}0>$ (b): reduced grain boundary mobility A_b (solid triangles) and reduced triple junction mobility A_{tj} (solid squares) [47].

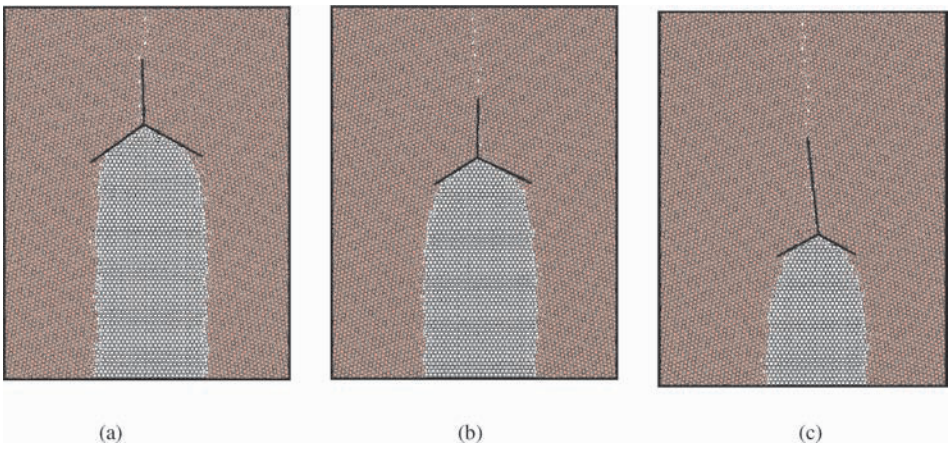

Figure 12 The atomic configuration of a φ=33° migrating triple junction for the "Fig. 6" simulation geometry at three instants of time: (a) $t = 550\tau$, (b) $t = 1245\tau$ and (c) $t = 2550\tau$. The bold lines indicate the tangents to the half-loop boundary at the triple junction. The dynamic triple junction angle was $\theta = 56°$ in (a) $\theta = 58°$ in (b) and $\theta = 58°$ in (c) [45].

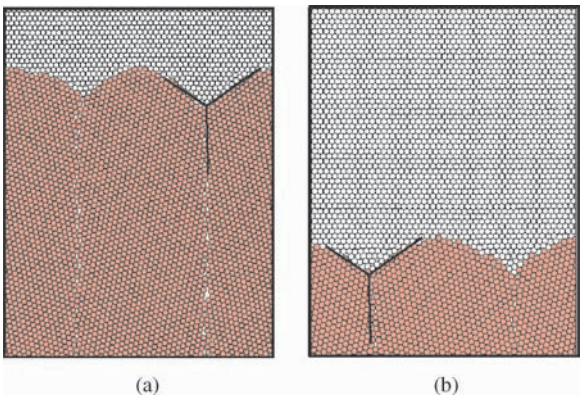

Figure 13 Same as in Fig. 10, but for the "Fig. 7" geometry. The atomic configurations correspond to instants of time: (a) $t = 2000\tau$ and (b) $t = 14000\tau$. The dynamic triple junction angle was $\theta = 61°$ in (a) and $\theta = 62°$ in (b) [45].

of non-equilibrium triple junction angles and substantial triple junction drag seen in recent experiments [41–43, 45–47].

In the light of the results discussed, it is of interest to consider the Von Neumann–Mullins relation. Actually, it was repeatedly pointed out that one of the three assumptions on which this relation is based is the requirement associated with triple junction mobility, namely the mobility of triple junctions should be infinitely large to establish equilibrium contact angles at triple junctions, which for uniform grain boundaries are equal to 120°. To conserve the central idea of the Von Neumann–Mullins relation let us consider a situation when the influence of the triple junction is rather large, but nevertheless, the motion of the system can be viewed as grain boundary motion, since the driving force is still due to the grain boundary curvature, i.e. the role of the triple junctions is reduced to a change of the angle θ. As mentioned above Equations 77 and 78 describe the steady state value of the angle θ. Clearly triple junctions in real polycrystals rarely experience steady state motion. However, the attainment of a true steady state is not important in this context. Even if the angle θ is not in steady state with the moving triple junction, it will be different from the equilibrium θ angle $\pi/3$ as assumed for the Von Neumann-Mullins relation and thus, will affect the kinetics with the same tendency as in steady state.

Since we consider the motion of a boundary driven by grain boundary curvature with a triple junction and due to the fact that triple junctions have their own mobility

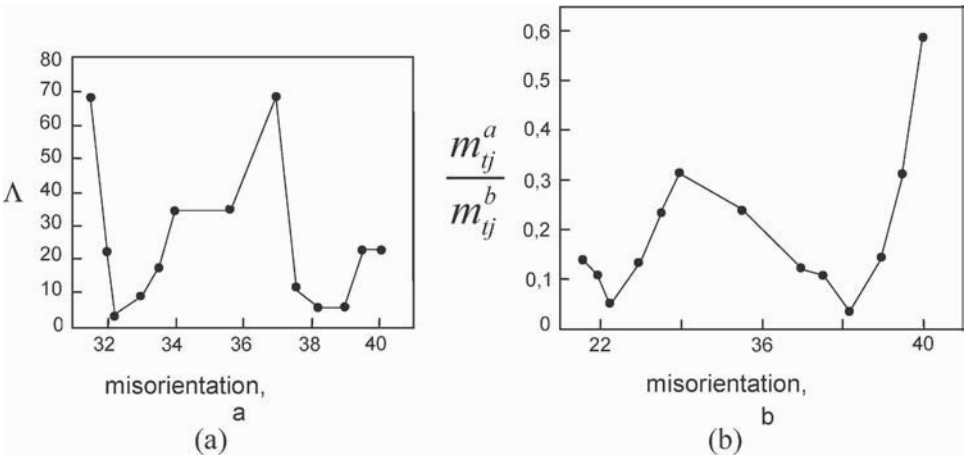

Figure 14 The misorientation dependence of Λ the simulations with geometry given in Fig. 6 at $T = 0.3\ T_m$ (a) [43] and the ratio $\frac{m^a_{tj}}{m^b_{tj}}$ of the triple junction mobility extracted for the simulation geometry shown in Fig. 6 (m^a_{tj}) and Fig. 7 (m^b_{tj}) [45].

the motion of such a boundary can be considered as a motion of a boundary with mobile defects [48]. That is why the rate of area change can be expressed as [48]:

$$\frac{dS}{dt} = -m_b\gamma_b \oint \frac{d\varphi}{1+\frac{1}{\Lambda}} = -\frac{A_b}{1+\frac{1}{\Lambda}} \oint d\varphi \quad (75)$$

Because the integral $\oint d\varphi$ for n-sided grains under the impact of a non-equilibrium contact angle is equal to [39] $\oint d\varphi = 2\pi - n(\pi - 2\theta)$ Equation 72 takes the form

$$\frac{dS}{dt} = -\frac{A_b}{1+\frac{1}{\Lambda}}\left[2\pi - n(\pi - 2\theta)\right] \quad (76)$$

Obviously the expression for the rate of area change will be different for grains with $n < 6$ and $n > 6$. Since the limited mobility of triple junction reduces the steady state value of the angle θ as compared to the equilibrium angle, the shrinking rate of the grains with $n < 6$ decreases. In other words, the influence of the triple junction evolution decreases the vanishing rate of grains with small topological classes.

Correspondingly, for grains with $n > 6$ the dragging influence of triple junction increases the angle θ and decelerates the process of grain structure evolution. In other words, microstructural evolution is slowed down due to triple junction drag for any n-sided grain. Since the actual magnitude of θ is determined by triple junction and grain boundary mobility as well as grain size there is no unique border between vanishing and growing grains with respect to their topological class anymore. Let us consider this situation in greater detail.

Inasmuch as we are approaching the migration of a grain boundary system with triple junction still as grain boundary motion even though the influence of it is rather large, the contact angle $\theta$is a function of the criterion Λ:$\theta = \theta(\Lambda)$. By considering this situation in the vicinity of the "equilibrium" state, ($\theta = \pi/3$) we can obtain the expression for $\theta = 0(\Lambda)$ in an explicit form [49]. Actually, expanding the function $2\cos\theta - 1$ into a power series in the vicinity of $\theta = \pi/3$ for $n < 6$ and $n > 6$, respectively, and neglecting terms above first order for $n < 6$, we arrive at:

$$2\theta = \Lambda(2\cos\theta - 1)) \cong \Lambda[(2\cos\theta - 1)_{\theta=\pi/3} + (-2\sin\theta)_{\theta=\pi/3}(\theta - \pi/3) + \cdots] \quad (77)$$

and, therefore,

$$\theta = \frac{\sqrt{3}\pi\Lambda}{6 + 3\sqrt{3}\Lambda} \quad (78)$$

and

$$\frac{dS}{dt} = \frac{m_b\gamma_b\pi}{3\left(1+\frac{1}{\Lambda}\right)}\left(n\frac{6+\sqrt{3}\Lambda}{2+\sqrt{3}\Lambda} - 6\right) \quad (79)$$

For $\Lambda \to \infty$—boundary kinetics regime—the expression (83) approaches the Von Neumann—Mullins relation. It is of particular interest to consider the topological class n^* of grains for which $\frac{dS}{dt} = 0$

$$n^* = \frac{2+\sqrt{3}\Lambda}{1+\frac{\sqrt{3}}{6}\Lambda} \quad (80)$$

Obviously, for $\Lambda \to \infty$ $n^* \to 6$ and n^* decreases for small Λ.

Let us consider the case for $n > 6$. From Equation 74

$$\frac{1}{\Lambda} = \frac{2\cos\theta - 1}{\ln\sin\theta} \cong \left(\frac{2\cos\theta - 1}{\ln\sin\theta}\right)_{\theta=\pi/3} + + \left[\frac{(-2\sin\theta)\ln\sin\theta - (2\cos\theta - 1)\cot\theta}{(\ln\sin\theta)^2}\right]_{\theta=\pi/3} \times (\theta - \pi/3) + \cdots \quad (81)$$

Finally, we arrive at

$$\frac{1}{\Lambda} = \left(-\frac{2\sin\theta}{\ln\sin\theta}\right)_{\theta=\pi/3}(\theta - \pi/3) = -\frac{\sqrt{3}}{\ln\sin\pi/3}(\theta - \pi/3)$$

or

$$\theta = \pi/3 + \frac{1}{\Lambda B}, \quad \text{where} B = -\frac{\sqrt{3}}{\ln \sin \pi/3} \tag{82}$$

and the expression for $\frac{dS}{dt}$ reads

$$\frac{dS}{dt} = \frac{m_b \gamma_b \pi}{3\left(1+\frac{1}{\Lambda}\right)}\left[n\left(1 - \frac{6}{\pi \Lambda B}\right) - 6\right] \tag{83}$$

As for $n < 6$, for $\Lambda \to \infty$ Equation 83 approaches the Von Neumann–Mullins relation. The value of n^* in this case is equal to

$$n^* = \frac{6}{1 - \frac{6}{\pi \Lambda B}} \tag{84}$$

For $\Lambda \to \infty$ n^* tends to the value 6, and n^* grows as Λ decreases.

It is seen that the drag effect of grain boundary triple junctions is manifested in an "increase" (in a topological sense) of shrinking grains and in a "decrease" of growing grains, respectively.

Let us examine the behavior $n^*(\Lambda)$ for $n < 6$ and $n > 6$. In Fig. 15 these values are denoted as $n^*_{\mathrm{L}}(\Lambda)$ and $n^*_{\mathrm{H}}(\Lambda)$, respectively. From the previous discussion it appears that grains with topological class between $n^*_{\mathrm{H}}(\Lambda)$ and $n^*_{\mathrm{L}}(\Lambda)$ are neither capable of growing nor of shrinking (Fig. 15). Hence, grains of the topological classes in the hatched area will be stable.

So far we have considered the motion of a grain boundary system with triple junctions in the case that the system moves under boundary kinetics while triple junctions only slightly disturb the motion of the system. In the following we consider the rate of change of a grain area S and peculiarities of grain growth when the motion of grain boundaries is controlled by the motion (mobility) of triple junctions. To begin with we will show that under triple junction control in the course of grain growth in 2D systems the grains will eventually be bordered by straight lines, i.e. they will assume a polygonal shape.

Let us consider the curvature of a grain boundary system with triple junctions (Figs 6 and 7). As shown in [43] for the system sketched in Fig. 6 we obtain with $\xi = \frac{a}{2\theta}$ for the local curvature of the boundaries

$$K = \frac{1}{\xi} e^{-x/\xi + \ln \sin \Theta} = \frac{2\Theta}{a} e^{-\frac{2\Theta}{a}x} \sin \Theta (2\cos\Theta - 1) e^{\frac{2\Theta}{a}x} \tag{85}$$

while for the geometry shown[‡] in Fig. 7

$$K = \frac{\ln \sin \Theta}{x_0} e^{\frac{x}{x_0} \ln \sin \Theta} = \frac{\Lambda}{x_0}(1 - 2\cos\Theta) e^{\frac{x}{x_0} \ln \sin \Theta} \tag{85a}$$

Since for triple junction kinetics $\Lambda \to 0$, also the grain boundary curvature K approaches zero, i.e. the grain structure of 2D polycrystals comprises straight grain boundaries which extend between the triple junctions. In other words, under triple junction kinetics the grains in a 2D polycrystal represent a system of polygons. More specifically, as shown in [48], in the framework of triple junction kinetics a polygon of arbitrary shape will be transformed in an equilateral polygon, and any deviation from an equilateral polygon will generate a force to restore the equilibrium shape. The only exception is a triangle. In other words a grain of topological class $n = 3$ is always unstable and must disappear. Finally, all other shrinking polygons must by necessity go though this stage eventually.

We reason that this phenomenon has important consequences for the development of grain growth [48]. Let us take a look at the evolution of a shrinking grain in the course of grain growth. The topological class of such a grain should be smaller than 6, naturally taking into account all corrections to the Von Neumann-Mullins relation, given above. As shown above the transition between boundary and triple junction kinetics does not only depend on grain boundary and triple junction mobility, but on the size of a grain as well. When the size of a grain diminishes progressively there comes a time where boundary kinetics becomes replaced by junction kinetics. This will happen to grains of the topological class $n = 4$ or $n = 5$ which are bound to shrink even after such a transition to triple junction kinetics. Grains of topological class $n = 3$ will collapse without transforming into a regular polygon. Since the kinetics of triple junctions is significantly slower than boundary kinetics, the four and five-side polygons will shrink, and eventually converge to a point although at a markedly smaller rate. Experimentally this phenomenon will manifest itself in the mean value of the topological class of vanishing grains. In Fig. 16 experimental data of grain growth in aluminum foil with 2D (columnar) structure is presented, in terms of the grain size dependence of the mean topological class $<n>$ [50, 51]. Extrapolation of this experimental dependence to zero area yields the mean value of the topological class of vanishing grains. As can be seen $<n>(0) = 4.2$ [45] and $<n>(0) = 4.0$ [46]

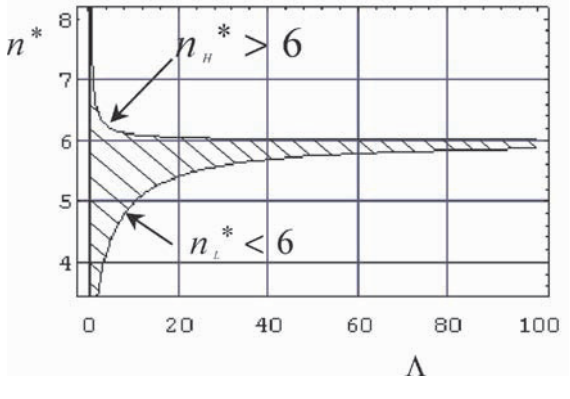

Figure 15 Functional dependency of $n^*_H(\Lambda)$ and $n^*_L(\Lambda)$ [49].

[‡] We note that for the grain boundary system presented in Fig. 7 triple junction control causes$\Theta \to \pi/2$.

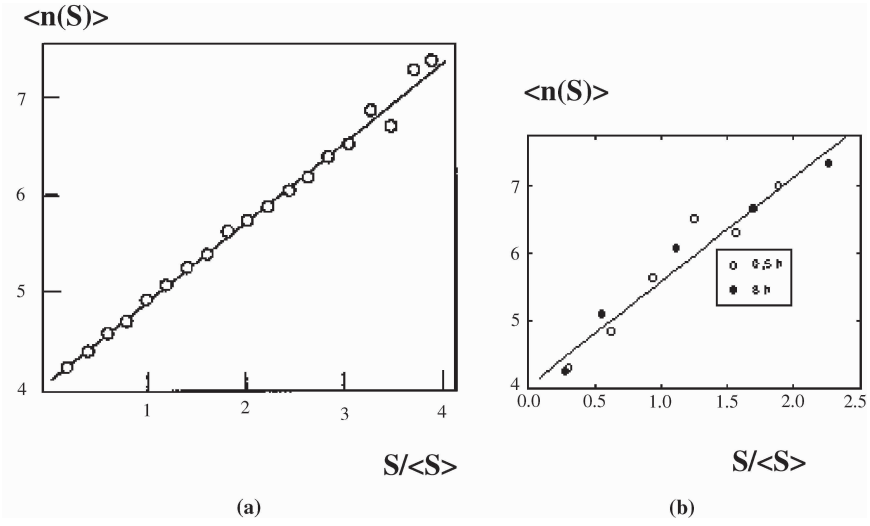

Figure 16 Dependence of the mean topological class $<n(s)>$ on "grain size" $s/<s>$ (normalized by the average grain size) in pure Al [50] (a), [51] (b).

respectively., i.e. $n = 4$ is the smallest topological class to shrink in a stable manner (Figs 16a and b).

Let us finally consider the behaviour of a regular n-sided polygon. The change of its area dS can be represented as [48]:

$$\frac{dS}{dt} = \oint V_{\mathrm{n}} dl = -V_{\mathrm{n}} \oint dl = -V_{\mathrm{n}} \Pi \qquad (86)$$

where V_{n} is the boundary velocity parallel to the boundary normal, Π is the perimeter of a polygon.

For a regular polygon

$$\begin{aligned} V_{\mathrm{n}} &= V_{\mathrm{TJ}} \cos(\pi/2 - \theta) \\ &= m_{\mathrm{Tj}} \gamma (2\cos\theta - 1)\cos(\pi/2 - \theta) \end{aligned} \qquad (87)$$

Since the angle θ for a regular n-sided polygon is equal to $\pi(n-2)/2n$, Equation 91 can be rewritten as

$$V_{\mathrm{n}} = m_{\mathrm{Tj}} \gamma [2\sin(\pi/n) - 1]\cos(\pi/n) \qquad (88)$$

where n is the topological class of the grain. From Equations 87 and 88 we obtain the rate of change of the grain area S, when grain boundary motion is controlled by the displacement of the triple junctions

$$\frac{dS}{dt} = -m_{\mathrm{Tj}} \gamma [2\sin(\pi/n) - 1]\cos(\pi/n)\Pi \qquad (89)$$

The perimeter of a regular n-sided polygon is equal to:

$$\Pi = 2n\tilde{R}\sin\left(\frac{\pi}{n}\right) = 2n\tilde{r}\tan\left(\frac{\pi}{n}\right) \qquad (90)$$

where $\tilde{R}$ is the radius of the circle circumscribing the polygon and $\tilde{r}$ is the radius of the circle inscribed into the polygon.

Then Equation 89 can be expressed as:

$$\begin{aligned} \frac{dS}{dt} &= -m_{Tj}\gamma n\tilde{R}\sin\left(\frac{2\pi}{n}\right)\left[2\sin\left(\frac{\pi}{n}\right) - 1\right] \\ &= -2m_{Tj}\gamma n\tilde{r}\sin\left(\frac{\pi}{n}\right)\left[2\sin\left(\frac{\pi}{n}\right) - 1\right] \end{aligned} \qquad (91)$$

In essence, therefore, a limited triple junction mobility always slows down the evolution of grain microstructure of polycrystals, irrespective whether the topological class of the considered grain is smaller or larger than 6. Formally, for grains with $n < 6$, the sluggish motion of the triple junction "reduces" the effective topological class of growing grains, while for grains with $n > 6$ the triple junction behavior "increases" the topological class of vanishing grains.

The mere fact that there is a growing grain with triple junctions of low mobility requires the existence of other grains with $n < 6$ to surround it. There is no point to discuss to which grain their common junction belongs.

The only exception holds for $n = 6$, since a hexagonal grain structure now becomes unstable even when the contact angle $2\theta = 2\pi/3$. Since the actual magnitude of Λ is determined by the triple junction and grain boundary mobility as well as the grain size and is independent of the number of sides of a grain, there is no unique dividing line between vanishing and growing grains with respect to their topological class anymore, like $n = 6$ in the Von Neumann-Mullins approach. As has been detailed above for sufficiently small Λ the border between shrinking and growing grains represents a region bounded by the lines $n^*_{\mathrm{H}}(\Lambda)$ and $n^*_{\mathrm{L}}(\Lambda)$ (Fig. 15) which degenerates to a line for $\Lambda \to \infty$.

As for the situation, when grain boundary migration is completely controlled by triple junction motion, it is interesting to compare the obtained Equation 91 with the Von Neumann–Mullins relation (72), which gives the rate of area change of a grain with topological class n under the condition that the triple junctions do not affect grain boundary motion. Evidently, the qualitative behaviour of Equations 91 and 72 is similar. Grains with $n > 6$ will grow while those with $n < 6$ disappear in

accordance with both Equations 72 and 91. What distinguishes Equations 91 and 72 is, firstly, the dependence of the rate of change on the topological class n. According to Equation 72, *dS/dt* increases infinitely with the number n, whereas for the triple junction kinetics, as can be extrapolated easily

$$\lim_{n\to\infty} \frac{dS}{dt} = 2\pi \bar{R} m_{tj} \gamma \tag{92}$$

The second distinctive difference is connected with the dependence of the rate of area change on the grain size. The Von Neumann–Mullins relation (79) does not depend on the grain size, whereas Equation 91 relates the rate of area change to the grain size.

In conclusions, an investigation into the effect of triple junction mobility on the rate of change of the grain area during 2D grain growth revealed that a finite junction mobility exerts a drag on the adjoining grain boundaries. This is reflected by a deviation of the grain vertex angles at triple junctions from their equilibrium value $2\pi/3$ and correspondingly, by a modification of the Von Neumann-Mullins relation. It was shown that for the situation when the triple junction influence on grain boundary motion is large enough, but nevertheless, grain boundary motion is controlled by grain boundary kinetics, the triple junction influence results in a reduced rate of microstructure evolution during grain growth, since the effective topological class of growing grains ($n > 6$) is decreased and of shrinking grains ($n < 6$) is increased. The triple junction influence creates a "topological range" of "stable" grains which are neither capable of growing nor of shrinking (Fig. 15).

It is stressed also that experimental results [50, 51] of the limiting topological class of disappering grains correlate both with the developed concepts of grain evolution in the course of grain growth controlled by triple junction kinetics and with the generalized form of the Von Neumann–Mullins relation.

Also, when grain boundary motion is controlled by the displacement rate of triple junctions, the Von Neumann–Mullins relation is replaced by a relation, that does not only take into account the topological class of a grain but its perimeter as well.

The considered problem and thus, the obtained relations, are relevant for the kinetics of general microstructure evolution in polycrystals, but especially in nanocrystalline systems, and in the case of abnormal grain growth.

7. Relative efficiency of different mechanisms on retardation of grain growth

Finally, we will proceed to the essential engineering problem: a comparison of the efficiency of the drag effects on grain growth [52].

The rate of grain area change $\frac{dS}{dt}$ of a grain is chosen as a measure of stability of a grain structure. It seems surprising to choose a rate as a measure of stability. The advantage of such a measure is evident: the change of grain area characterizes grain growth to a greater extent than the change of grain size which can be distinctly different even for the same grain. We shall consider the problem for 2D polycrystalline structures. Doubtlessly, most materials do not represent 2D systems. However the concepts of grain growth on the basis of boundary and junction migration were elaborated best for 2D systems. Further, for the value $\frac{dS}{dt}$ there is a strict Von Neumann-Mullins relation for the uniform boundary approach, and a corresponding relation [48] for junction controlled grain growth. If the velocity of grain boundary motion V is known we can express the rate of grain area change $\frac{dS}{dt} = \frac{d}{dt}(\bar{R}^2) = 2\bar{R}\frac{d\bar{R}}{dt} = 2\bar{R}V$, where $2\bar{R}$ is a mean grain size. Finally, since we are interested in the relative efficiency on grain growth retardation a 2D approach is physically adequate.

Let's consider the relative efficiency of different structural elements and defects of a polycrystal on grain growth. For this, we will use a ranking of the dimensionless criterion λ_{ik},

$$\lambda_{i,k} = \frac{\left(\frac{dS}{dt}\right)_i}{\left(\frac{dS}{dt}\right)_k} \tag{93}$$

which constitute a ratio of the rate of grain area change for different regimes and drag mechanisms. For instance, the situation $\lambda_{ik} < 1$ signifies that grain growth is controlled by mechanism (i) and the magnitude of λ_{ik} determines the efficiency of the drag.

7.1. Impurity drag

For grain boundary kinetics the rate of grain area change $\frac{dS}{dt}$is expressed by the Von Neumann–Mullins relation (72). The influence of impurities is effectively reflected in the grain boundary mobility $m_b(c)$, where c is the concentration of the impurities. The criterion λ_{imp}, 0 in this case is equal to:

$$\lambda_{imp,0} = \frac{\left(\frac{dS}{dt}\right)_{imp}}{\left(\frac{dS}{dt}\right)_{C=0}} = \frac{\frac{m_b(c)\gamma_b\pi}{3}(n-6)}{\frac{m_b\gamma_b\pi}{3}(n-6)} = \frac{m_b(c)}{m_b} \tag{94}$$

where $(\frac{dS}{dt})_{C=0}$ and $(\frac{dS}{dt})_{imp}$ are the rate of grain area change in a "pure" metal and in a metal with impurities, respectively. As the mobility depends strongly on the crystallographic parameters of a grain boundary the most correct way to define $\lambda_{imp,0}$ is to use data for specific and defined grain boundaries with different amount of impurities. For instance, for a <111> tilt grain boundary (misorientation angle 38.2° (Σ7)) in Al with total impurity content 0.4 ppm and 7.0 ppm, respectively, at 200°C the criterion $\lambda_{imp,0}$ is equal to $5 \cdot 10^{-4}$. For a non-special grain boundary <111> (misorientation angle 40.5°) at the same temperature $\lambda_{imp,0} = 1.7 \cdot 10^{-4}$ [53].

Unfortunately, the number of corresponding experimental studies is extremely small. On the other hand materials engineers are interested in the so called "average" grain boundary. As a first approximation we propose to use a combination of the Burke-Turnbull

expression for the grain boundary velocity [54]

$$V = \frac{b\nu\Omega_a P}{kT}\exp\left(-\frac{H_m}{kT}\right) \tag{95}$$

(b: atomic spacing, ν: Debye frequency, H_m: activation enthalpy of grain boundary motion) and the Lücke-Detert approximation which takes into account the effect of impurities on grain boundary mobility:

$$m_b = \frac{D_0 \exp\left(-\frac{(H_{Dimp}+H_{int})}{kT}\right)}{N_a B_0 kT \cdot c} \tag{96}$$

where D_0: preexponential factor of the diffusion coefficient, H_{Dimp}: activation enthalpy for bulk diffusion of impurity atoms, H_{int}: interaction energy of impurity atoms with the boundary, N_a: number of adsorption sites in the grain boundary, B_0: preexponential factor of the adsorption coefficient, c: bulk impurity concentration.

With the approximation $H_m = H_{SD}$, we arrive at:

$$\lambda_{imp,0} = \frac{D_0 \exp\left(-\frac{(H_{Dimp}-H_{SD}+H_{int})}{kT}\right)}{N_a B_0 \Omega_a b\nu \cdot c} \tag{97}$$

For instance, let us consider Fe as an impurity in aluminum. Then $D_0 = 91$ m^2/s, H_{dimp} = 2.68eV; $H_{SD} = 1.48$eV [55]; $H_{int} \cong 0.24$eV [56, 10]; $V_a \approx 5.10^{-5}$ mol/m^2; $\Omega_a \approx$ 10-5 m^3/mol; $B_0 = 1$; $b = 3 \cdot 10^{-10}$m; $n = 10^{13}$. Then for $c \approx 10^{-5}$ at 200°C $\lambda_{imp,0} \approx 3.6 \cdot 10^{-3}$.

It is advisable to point out that grain boundary absorption decreases with decreasing grain size what makes impurity drag less effective.

7.2. Triple junction drag

In this instance we compare the rate of area change as affected by triple junction drag compared to free uniform boundary motion.

$$\lambda_{tj,b} = \frac{\frac{dS}{dt}\big|_{tj}}{\frac{dS}{dt}\big|_{b}} = \frac{-m_{tj}\gamma_b \bar{R} n \sin\left(\frac{2\pi}{n}\right)\left[2\sin\left(\frac{\pi}{n}\right)-1\right]}{\frac{m_b\gamma\pi}{3}(n-6)} \tag{98}$$

where $\bar{R}$ is the grain size. As shown in [48], triple junction kinetics cause a polygon of arbitrary shape to be transformed into an equilateral polygon, and any deviation from an equilateral polygon will generate a force to restore the equilibrium shape.

For the average topological class of a 2D system, namely for $\bar{n} = 6$. $\lambda_{tj,b}$ is indefinite, but with the L'Hôpital's rule

$$\lambda_{tj,b} = \lim_{n\to 6}\frac{\frac{d}{dn}\left(\frac{dS}{dt}\right)_{tj}}{\frac{d}{dn}\left(\frac{dS}{dt}\right)_{b}} = \frac{3}{4}\frac{m_{tj}\bar{R}}{m_b} = \frac{3}{4}\Lambda \tag{99}$$

A distinctive property of the expressions (98) and (99) is the explicit dependency of λ on the grain size.

Unfortunately, grain boundary triple junction mobility has been explored very poorly. Using experimental data [42] for a triple junction formed by ⟨111⟩ tilt grain boundaries in pure Al, $\bar{R} = 10^{-8}$ m and 200°C and 300°C, we obtain $\Lambda = 10^{-12}$ and $\Lambda = 4{\cdot}10^{-10}$, respectively. For another investigated triple junction formed by the same tilt boundary system (with misorientation angles different from previous case) the values $\Lambda$for $\bar{R} = 10^{-8}$ m at 200°C and 300°C are equal to $\Lambda = 10^{-11}$ and 10^{-8} respectively. In other words, the efficiency of triple junction dragging for $R = 10^{-8}$ m at 200°C: $\lambda_{tj-b(200°C)} \approx 10^{-12}$ and $\lambda_{tj,b}$ (200°C) $\approx 10^{-11}$, at 300°C: $\lambda_{tj,b}$ (300°C) $\approx \cdot 10^{-9}$ and $\lambda_{tj,b}$ (300°C) $\approx 10^{-8}$, respectively. As a result triple junctions constitute a powerful drag factor against grain growth in nanocrystalline materials.

To illustrate the drag power of triple junctions it is helpful to discuss experimental work of a "direct" comparison of the mobility of a grain boundary system with and without a triple junction [47]. Actually, the configuration (Fig. 6) without a triple junction constitutes a grain boundary half-loop, the theory and experimental features of which are well elaborated [10]. The motion of a grain boundary half-loop in Zn of 99.995% purity was studied. In addition, the motion of practically the same half-loop with a low-angle straight boundary in configuration Fig. 6 was investigated. "Practically the same" means that the incorporation of the low-angle grain boundary changes the misorientation of the curved grain boundaries only very moderately. Hence, we can conduct a "direct" comparison between the motion of a grain boundary half-loop and the motion of the "same" half-loop with a triple junction. Two tilt grain boundary systems were studied: 84° ⟨11$\bar{2}$0⟩ and 62° ⟨10$\bar{1}$0⟩. In the triple junction configuration the misorientation of the straight boundary in both cases was about 3°. The dependency of the reduced displacement *al(t)* on time is given for both configurations in Fig. 17. By definition $a\ell(t) = a \cdot \ell(t)$, where a is the width of the half loop and $\ell(t)$ is displacement with time, takes automatically care of a changing width of the half loop, i.e. is independent of the driving force λ/a. The experimented results demonstrate the strong drag of the triple junction on the motion of the grain boundary system [47].

7.3. Vacancy injection drag

With the expression for the effective velocity of grain growth under the influence of ejected vacancies Equation 40 the effective mobility of grain boundaries can be expressed as:

$$m_{beff} = \frac{V_{eff}}{P} = \frac{1}{36}\cdot\frac{RD_{SD}}{NkTZ(\beta\delta)^2} \tag{100}$$

where $P = \frac{\gamma}{\bar{R}}$ is a driving force for grain growth. Comparing this with boundary motion unaffected by

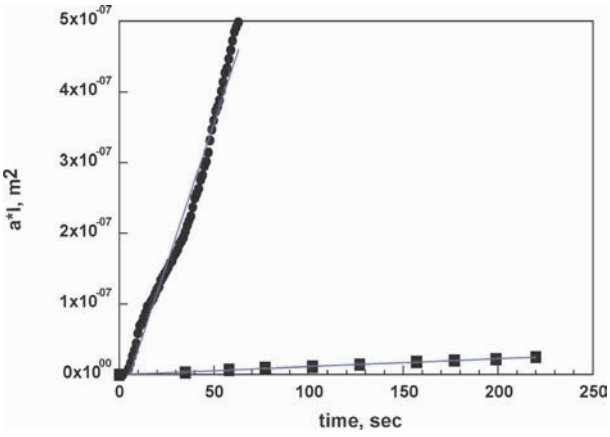

Figure 17 Time dependence of reduced displacement $al(t)$ for $\langle 11\bar{2}0\rangle$ tilt grain boundary half-loop (solid circles) and triple junction configuration (solid squares) at $T = 390^{\circ}$C [47].

vacancy supersaturation we define the criterion

$$\lambda_{\mathrm{vac,b}} = \frac{m_{\mathrm{beff}}\gamma\pi(n-6)}{3} \Big/ \frac{m_{\mathrm{b}}\gamma\pi(n-6)}{3} = \frac{1}{36}\cdot\frac{D_{\mathrm{SD}}}{A_{\mathrm{b}}}\frac{\bar{R}\gamma}{NkTZ(\beta\delta)^2} \tag{101}$$

where A_{b} is the reduced mobility of grain boundaries: $A_{\mathrm{b}} = m_{\mathrm{b}}\gamma$. For pure Al at 300°C using the experimental data of grain boundary mobility [10] $\lambda_{\mathrm{vac,b}} \approx 10^3 R$, and with $\bar{R}$ in the order of $10^{-8}m$ $\lambda_{\mathrm{vac,b}} \approx 10^{-5}$.

7.4. Particle drag

Two types of particle drag have to be considered: the dragging by small mobile particles and large immobile particles. However, the grain size in nanostructures is so small that the existence of large immobile particles is difficult to imagine, since by common understanding the particle size has to be smaller than the grain size. That is why we will only consider the joint motion of grain boundaries together with the particles. The effective mobility of a grain boundary moving together with the particles was derived (Equation 26):

$$m_{\mathrm{eff}} = \frac{m_{\mathrm{p}}(r_0)}{n_0} \tag{102}$$

where $m_{\mathrm{p}}(r_0)$ and n_0 are the mobility of particles of radius r_0 and n_0 is the number of particles per unit area of the boundary, respectively. With Equations 26–31 and the approach used above we arrive at

$$\lambda_{\mathrm{part,b}} = \frac{\frac{dS}{dt}\big|_{\mathrm{part}}}{\frac{dS}{dt}\big|_{\mathrm{b}}} = \frac{m_{\mathrm{beff}}}{m_{\mathrm{b}}} = \frac{m_{\mathrm{p}}(r)}{n}\cdot\frac{1}{m_{\mathrm{b}}} = \frac{2}{3}\cdot\frac{\delta}{r^2}\cdot\frac{D_{\mathrm{S}}\Omega_{\mathrm{a}}}{kTm_{\mathrm{b}}}\cdot\frac{c_{\mathrm{B}}-c_{\mathrm{A}}}{c_0-c_{\mathrm{A}}} \tag{103}$$

With the parameters $\delta \approx 10^{-9}$ m; $D_{\mathrm{S}} \approx 10^{-10}$ m^2 s^{-1} [57]; $\Omega_{\mathrm{a}} \approx 10^{-5}$ m^3 mol^{-1}: $\gamma_{\mathrm{b}} \approx 1J\cdot m^{-2}$; $T = 573$ K; $c_{\mathrm{B}} = 1$; $c_{\mathrm{A}} = 10^{-4}$; $c_0 = 10^{-3}$; $A_{\mathrm{b}} \approx 10^{-10}$ m^{2}s^{-1} [10], $T = 200^{\circ}$C, we arrive at $\lambda_{\mathrm{part,b}} \simeq \frac{10^{-15}m^2}{r^2}$. In other words only sufficiently "large" particles will exert an efficient drag on grain growth in nanocrystalline systems.

It is of interest to consider the relative efficiency of particles and triple junctions on retardation of grain growth. We will consider the most "favourable" case for particles, their highest possible velocity of motion together with the grain boundary, i.e., the situation when the force acting on the particle balances the bonding force between the particle and the boundary:

$$V = m_{\mathrm{p}}(r_0)f_{\mathrm{p}}(r_0),\ f_{\mathrm{p}}(r) = \frac{3}{2}\pi r_0\gamma_{\mathrm{b}}.$$

With the approach repeatedly used above we obtain the mobility of a grain boundary migrating together with the particles at their maximum speed:

$$m_{\mathrm{beff}} = \frac{V}{P} = \pi m_{\mathrm{p}}(r_0)r_0\bar{R} \tag{104}$$

Consequently, the relative efficiency of triple junction drag compared to mobile particle drag can be expressed as:

$$\lambda_{\mathrm{tj-p}} = \frac{3}{4}\frac{m_{\mathrm{tj}}\bar{R}}{m_{\mathrm{beff}}} = \frac{3}{4}\frac{m_{\mathrm{tj}}}{\pi m_{\mathrm{p}}(r_0)r_0} \tag{105}$$

With the same values of the parameters used in Equation 103 and the reduced triple junction mobility $\gamma_{\mathrm{b}}m_{\mathrm{tj}} \approx 5.6\cdot 10^{-13}ms^{-1}$[42] for 300°C in Al we arrive at:

$$\lambda_{\mathrm{tj,part}} \approx 2\cdot 10^{15}m^{-3}\cdot r^3 \tag{106}$$

One can see that triple junction drag becomes comparable with particle drag only for $r \geq 10^{-5}m$, in other words for very large particles, ($r > 10\ \mu$m). In essence, the triple junction most effectively drag grain boundary motion in nanocrystalline materials.

8. Conclusions

The thermodynamic and kinetic aspects of grain growth and grain microstructure evolution in fine grained and nanocrystalline materials were considered. It was shown that neither impurities nor structural elements of a polycrystal can suppress grain growth completely, but under certain conditions they will slow down the process drastically.

A finite mobility of grain boundary triple junctions changes substantially our concepts of grain structure evolution in the course of grain growth.

The relative efficiency of the drag effect by different elements and defects of a polycrystalline microstructure was considered. Triple junction drag was found to be most effective for microstructural stabilization of very fine grained microstructures. We propose to use the derived hierarchy of dragging efficiency as an effective tool for grain boundary engineering of granular microstructures.

Acknowledgements

Support from the Deutsche Forschungsgemeinschaft (DFG Grant 436 RUS 113/714/0-1(R)) is gratefully acknowledged. One of the authors (LSS) wishes to thank the Russian Foundation of Fundamental Research for financial support (Grant DFG-RRFI 03 02 04000).

References

1. T. WATANABE, H. FUJII, H. OIKAWA and K. I. ARAI, *Acta Metall.* **37** (1989) 47.
2. T. WATANABE and S. TSUREKAWA, *Acta Mater.* **47** (1999) 4171.
3. T. WATANABE, "Recrystallization and Grain Growth", edited by G. Gottstein and D. A. Molodov, (Springer-Verlag, 2001) Vol. I, p. 11.
4. K. T. AUST, U. ERB and G. PALUMBO, *Mater. Sci. Engn.* **A176** (1994) 329.
5. E. M. LENOCKEY, G. PALUMBO, P. LIN and A. BRENNENSTUHL, *Metall. Mater. Trans.* **A29** (1998) 387.
6. R. KIRCHHEIM, *Acta Mater.* **50** (2002) 413.
7. A. MICHELS, C. E. KRILL, H. EHRHARDT, R. BIRRINGER and D. T. WU, *ibid.* **47** (1999) 2143.
8. J. E. BURKE, *Trans. Metall. Soc. A.I.M.E.* **175** (1949) 73.
9. E. RABKIN, *Scripta Mater.* **42** (2000) 1199.
10. G. GOTTSTEIN and L. S. SHVINDLERMAN, " Grain Boundary Migration in Metals: Thermodynamics, Kinetics, Applications" (CRC Press, 1999) p. 385.
11. G. GOTTSTEIN and L. S. SHVINDLERMAN, *Acta Metall. Mater.* **41** (1993) 3267.
12. L. S. SHVINDLERMAN and G. GOTTSTEIN, *Scripta Mater.* **50** (2004) 1051.
13. D. A. MOLODOV, U. CZUBAYKO, G. GOTTSTEIN and L. S. SHVINDLERMAN, *Acta Mat.* **46** (1998) 553.
14. C. S. SMITH, *Trans. A.I.M.E.* **175** (1948) 15.
15. Y. ESTRIN, G. GOTTSTEIN and L. S. SHVINDLERMAN, *Scripta Mater.* **41** (1999) 385.
16. *Idem.*, *ibid.* **41** (1999) 415.
17. *Idem.*, *Acta Mater.* **47** (1999) 3541.
18. Y. ESTRIN, G. GOTTSTEIN, E. RABKIN and L. S. SHVINDLERMAN, *Scripta Mater.* **43** (2000) 141.
19. *Idem.*, *Acta Mater.* **49** (2001) 673.
20. YA. E. GEGUZIN, "Physik des Sinterns" (VEB Deutscher Verlag für Grundstoffindustrie, Leipzig, 1973).
21. D. WOLF and K. L. MERKLE, in "Material Interfaces" edited by D. Wolf and S. Yip (Chapman & Hall, London, 1992) p. 87.
22. M. UPMANYU, D. J. SROLOVITZ, G. GOTTSTEIN and L. S. SHVINDLERMAN, *Interface Sci.* **6** (1998) 289.
23. K. LÜCKE and G. GOTTSTEIN, *Acta Metall.* **29** (1981) 779.
24. Y. ESTRIN and K. LÜCKE, *ibid.* **29** (1981) 791.
25. C. E. KRILL and R. BIRRINGER, in "Recrystallization and Grain Growth" edited by G. Gottstein and D. A. Molodov (Springer-Verlag, 2001) Vol. I, p. 205.
26. W. GUST, D.Sc. Thesis, University of Stuttgart, 1980.
27. A. H. KING, *Int. Mater. Rev.* **32** (1987) 173.
28. V. SEMENOV, E. RABKIN, E. BISCHOFF and W. GUST, *Acta Mater.* **46** (1998) 2289.
29. W. W. MULLINS, *J. Appl. Phys.* **28** (1957) 333.
30. F. Y. GENIN, *ibid.* **77** (1995) 5130.
31. P. CHAUDHARI, *J. Vac. Sci. Techn.* **9** (1972) 520.
32. C. V. THOMPSON and R. CAREL, *J. Mech. Phys. Sol.* **44** (1996) 657.
33. K. LÜCKE, I. HECKELMANN and G. ABBRUZZESE, *Acta Metall. Mater.* **40** (1992) 533.
34. M. P. ANDERSON, D. J. SROLOVITZ, G. S. GREST and P. SAHNI, *Acta Metall.* **32** (19 84) 783.
35. V. E. FRADKOV, L. S. SHVINDLERMAN and D. G. UDLER, *Scripta Metall.* **19** (1985) 1285.
36. V. E. FRADKOV and L. S. SHVINDLERMAN, "Structure and Properties of Interfaces in Metals" (Moscow, "Nauka", 1988) p. 213.
37. J. VON NEUMANN, "Metal Interfaces" (Americal Society for Testing Materials, Cleveland, 1952) p. 108.
38. W. W. MULLINS, *J. Appl. Phys.* **27** (1956) 900.
39. G. GOTTSTEIN and L. S. SHVINDLERMAN, *Scripta Mater.* **38** (1998) 1541; **39** (1998) 1489.
40. G. GOTTSTEIN, A. H. KING and L. S. SHVINDLERMAN, *Acta Mater.* **48** (2000) 397.
41. U. CZUBAYKO, V. G. SURSAEVA, G. GOTTSTEIN and L. S. SHVINDLERMAN, *ibid.* **46** (1998) 5863.
42. S. G. PROTASOVA, G. GOTTSTEIN, D. A. MOLODOV, V. G. SURSAEVA and L. S. SHVINDLERMAN, *ibid.* **49** (2001) 2519.
43. M. UPMANYU, D. J. SROLOVITZ, L. S. SHVINDLERMAN and G. GOTTSTEIN, *Interface Sci.* **7** (1999) 2307.
44. M. UPMANYU, D. J. SROLOVITZ, L. S. SHVINDLERMAN and G. GOTTSTEIN, *Acta Mater.* **47** (1999) 3901.
45. *Idem.*, *ibid.* **50** (2002) 1405.
46. L. S. SHVINDLERMAN, G. GOTTSTEIN, D. A. MOLODOV and V. G. SURSAEVA, in "Recrystallization and Grain Growth" edited by G. Gottstein and D. A. Molodov (Springer-Verlag, 2001) Vol. I, p. 177.
47. V. G. SURSAEVA, G. GOTTSTEIN and L. S. SHVINDLERMAN, in "Recrystallization and Grain Growth" edited by G. Gottstein and D. A. Molodov, (Springer-Verlag, 2001) Vol. I, p. 455.
48. G. GOTTSTEIN and L. S. SHVINDLERMAN, *Acta Mater.* **50** (2002) 703.
49. G. GOTTSTEIN, MIN ZENG, L. S. SHVINDLERMAN and Z. METALLKD, to be published.
50. V. E. FRADKOV, A. S. KRAVCHENKO and L. S. SHVINDLERMAN, *Scripta Metall.* **19** (1985) 1291.
51. V. G. SURSAEVA and S. G. PROTASOVA, in "Recrystallization and Grain Growth" edited by G. Gottstein and D. A. Molodov (Springer-Verlag, 2001) Vol. I, p. 327.
52. G. GOTTSTEIN, Y. ESTRIN and L. S. SHVINDLERMAN, *Acta Mater.* to be published.
53. D. A. MOLODOV, U. CZUBAYKO, G. GOTTSTEIN and L. S. SHVINDLERMAN, *ibid.* **46** (1998) 553.
54. J. E. BURKE and D. TURNBALL, *Progress Met. Phys.* **3** (1952) 220.
55. "Smithells Metalls Reference Book" Sixth edition (Butterworths, 1983, London).
56. D. A. MOLODOV, CH. V. KOPETSKII and L. S. SHVINDLERMAN, *Sov. Phys. Solid State* **23** (1981) 1718.
57. S. PROKOFJEV, V. ZHILIN, E. JOHNSON, M. LEVINSEN, J. S. ANDERSEN, U. DAHMEN, T. RADETIC and J. TURNER, in "Proc. VIII Seminar Diffusion and Thermodynamics of Materials" edited by J. Cermak and J. Vrest'al (Masarik University, Brno, 2002) p. 241.